

A 1-PARAMETER APPROACH TO LINKS IN A SOLID TORUS

T. FIEDLER AND V. KURLIN

ABSTRACT. To an oriented link in a solid torus we associate a trace graph in a thickened torus in such a way that links are isotopic if and only if their trace graphs can be related by moves of finitely many standard types. The key ingredient is a study of codimension 2 singularities of link diagrams. For closed braids with a fixed number of strands, trace graphs can be recognized up to equivalence excluding one type of moves in polynomial time with respect to the braid length.

1. INTRODUCTION

1.1. Motivation and summary.

The classical Reidemeister theorem says that plane diagrams represent isotopic links in 3-space if and only if they can be related by finitely many moves of 3 types corresponding to the codimension 1 singularities of links diagrams, namely a triple point \times , simple tangency χ and ordinary cusp γ .

We establish the higher order Reidemeister theorem considering a canonical 1-parameter family of links in a solid torus and studying codimension 2 singularities of resulting link diagrams. The 1-parameter family of link diagrams is encoded by a new combinatorial object, a trace graph in a thickened torus in such a way that *trace graphs determine families of isotopic links if and only if they can be related by a finite sequence of the 11 moves in Figure 11*, see Theorem 1.4.

The conjugacy problem for braids is equivalent to the isotopy classification of closed braids in a solid torus. Braids are *conjugate* if and only if the trace graphs of their closures are *equivalent* through only tetrahedral moves and trihedral moves in Figure 11i, 11xi. Trace graphs of closed braids can be recognized up to isotopy in a thickened torus and trihedral moves in polynomial time with respect to the braid length, see Theorem 1.5. The method provides a new geometric approach to the conjugacy problem for braid groups B_n , which still has no efficient solution for $n \geq 5$ strands, ie with a polynomial complexity in the braid length. Very promising steps towards a polynomial solution were made by Birman, Gebhardt, González-Meneses [3] and Ko, Lee [11]. A clear obstruction is that the number of different conjugacy classes of braids grows exponentially even in B_3 , see Murasugi [13].

Usually links are studied in terms of braids using the theorems of Alexander and Markov, see Birman [2]. The 1-parameter approach is a geometric alternative to the algebraic one: conjugacy of braids and Markov moves are replaced by a stronger notion of link isotopy and extreme tangency moves in Figure 11viii, respectively.

Date: October 18, 2008, the last version is available on www.durham.ac.uk/~dma0vk.

2000 Mathematics Subject Classification. 57R45, 57M25, 53A04.

Key words and phrases. Knot, braid, singularity, bifurcation diagram, trace graph, diagram surface, canonical loop, trihedral move, tetrahedral move.

1.2. Basic definitions.

We work in the C^∞ -smooth category. Fix Euclidean coordinates x, y, z in \mathbb{R}^3 . Denote by D_{xy} the unit disk with centre at the origin of the horizontal plane XY . Introduce the *solid torus* $V = D_{xy} \times S_z^1$, where the oriented circle S_z^1 is the segment $[-1, 1]_z$ with the identified endpoints, see the left picture of Figure 1.

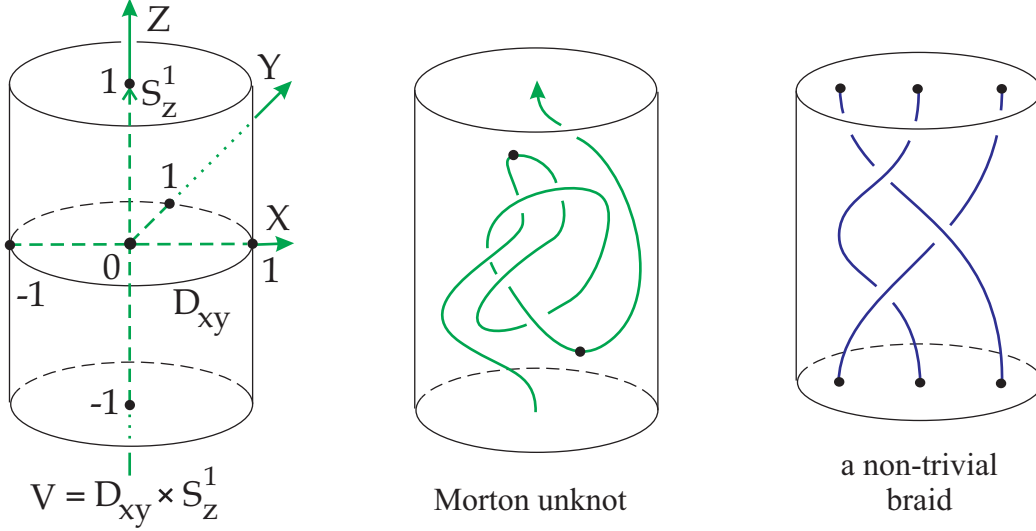


FIGURE 1. Basic notations and examples

Definition 1.1. An *embedding* is a diffeomorphism onto its image. An *oriented link* $K \subset V$ is the image of an embedding $f : \sqcup_{j=1}^m S_j^1 \rightarrow V$. An *isotopy* between two oriented links K_0 and K_1 in V is a smooth map $F : (\sqcup_{j=1}^m S_j^1) \times [0, 1] \rightarrow V$ such that $f_0(\sqcup_{j=1}^m S_j^1) = K_0$, $f_1(\sqcup_{j=1}^m S_j^1) = K_1$ and the maps $f_r = F(*, r) : \sqcup_{j=1}^m S_j^1 \rightarrow V$ are smooth embeddings for all $r \in [0, 1]$.

Mark n points $p_1, \dots, p_n \in D_{xy}$. A *braid* β on n strands is the image of a smooth embedding of n segments into $D_{xy} \times [-1, 1]_z$ such that (see Figure 1)

- the strands of β are monotonic with respect to $\text{pr}_z : \beta \rightarrow S_z^1$;
- the lower and upper endpoints of β are $\cup(p_i \times \{-1\})$, $\cup(p_i \times \{1\})$, respectively.

Braids are considered up to isotopy in the cylinder $D_{xy} \times [-1, 1]_z$, fixed on its boundary. The isotopy classes of braids form the group denoted by B_n . The *trivial* braid consists of n vertical segments $\sqcup_{i=1}^n (p_i \times [-1, 1]_z)$. A braid $\beta \in B_n$ is *pure* if the induced permutation $\tilde{\beta} \in S_n$ is its endpoints is trivial. The *closed* braid $\hat{\beta} \subset V$ is obtained from $\beta \subset D_{xy} \times [-1, 1]_z$ by identifying the bases $\{z = \pm 1\}$. ■

The smoothness of a link K implies that the tangent vector $\dot{f}(s)$ never vanishes on K . The *standard* unknot is given by the trivial embedding $S_z^1 \rightarrow V = D_{xy} \times S_z^1$. We introduce a new equivalence relation, *strong isotopy*, for links in a solid torus. For closed braids, the usual isotopy through closed braids is strong.

Definition 1.2. An *extreme pair* of a link $K \subset V$ is a pair of either 2 local maxima $\wedge\wedge$ or 2 local minima $\vee\vee$ of the projection $\text{pr}_z : K \rightarrow S_z^1$ with the same z -coordinate. A smooth isotopy $F : (\sqcup_{j=1}^m S_j^1) \times [0, 1] \rightarrow V$ of links is called *strong* if all links in the family $K_r = F(\sqcup_{j=1}^m S_j^1, r) \subset V$ have **no** extreme pairs for $r \in [0, 1]$. ■

H. Morton proposed the trivial knot in the middle picture of Figure 1. The *Morton* unknot is not strongly isotopic to the *standard* unknot S_z^1 . The arc between the marked extrema is a long trefoil that can not be unknotted by strong isotopy since the marked extrema remain the highest and lowest critical points.

1.3. Trace graphs of links.

Links are usually represented by plane diagrams with double crossings. A classical approach to the classification of links is to use isotopy invariants, ie functions defined on plane diagrams and invariant under the Reidemeister moves. The Reidemeister moves in Figure 5 correspond to simplest singularities that can appear in diagrams of links under isotopy, eg Reidemeister move III describes the change of a diagram when a transversal triple intersection \times appears in the projection.

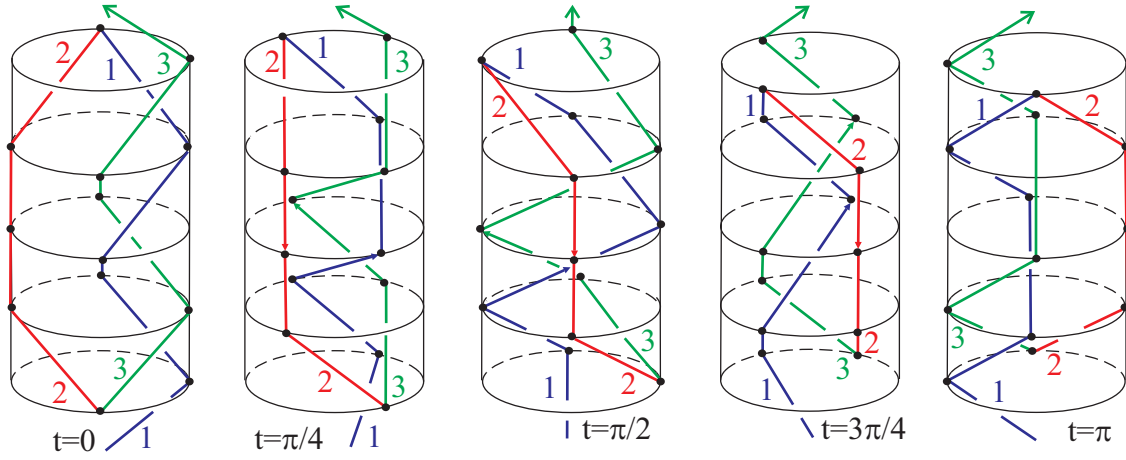


FIGURE 2. Diagrams of rotated trefoils $\text{rot}_t(K) \subset V$ for $t \in [0, \pi]$

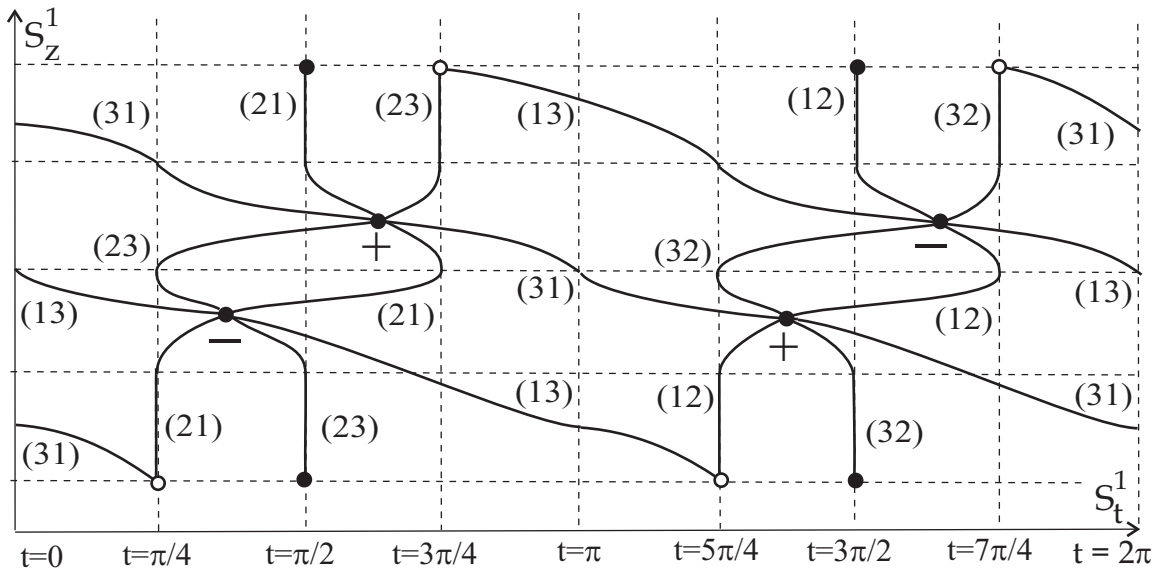


FIGURE 3. The trace graph $\text{TG}(K)$ obtained from the diagrams in Figure 2.

The analogue of a plane diagram in the 1-parameter approach is a 1-parameter family of diagrams obtained by rotating a link in V around S_z^1 . This is a 2-dimensional surface containing more information about the link than only one plane diagram. The link will be reconstructed up to smooth equivalence from the self-intersection of the surface, the *trace graph*. Denote by $\text{rot}_t : V \rightarrow V$ the *rotation* of the torus V around S_z^1 through an angle $t \in [0, 2\pi)$, see Figure 2. Here t is the parameter on *the time circle* $S_t^1 = \mathbb{R}/2\pi\mathbb{Z}$ of length 2π . Let A_{xz} be the vertical annulus $[-1, 1]_x \times S_z^1$ in the solid torus V . Define the *thickened torus* $\mathbb{T} = A_{xz} \times S_t^1$. We illustrate the rotation of V using the piecewise linear trefoil $K \subset V$ in Figure 2, which can be easily smoothed. Diagrams of rotated trefoils $\text{rot}_t(K) \subset V$ under the orthogonal *projection* $\text{pr}_{xz} : V \rightarrow A_{xz}$ are shown in Figure 2.

Definition 1.3. The *trace graph* $\text{TG}(K) \subset \mathbb{T}$ of a link $K \subset V$ consists of the crossings of the diagrams $\text{pr}_{xz}(\text{rot}_t(K))$ over all $t \in S_t^1$. Mark the intersection points from $K \cap (D_{xy} \times \{\pm 1\}) \subset V$ and also mark each local extremum of K with respect to $\text{pr}_z : K \rightarrow S_z^1$. If K has m components, in general position, the i -th component decomposes into n_i vertically monotonic arcs labelled by A_{iq} , $q = 1, \dots, n_i$. The 3 monotonic arcs in Figure 2 are numbered simply by 1, 2, 3.

Take a point $p \in \text{TG}(K)$, which is a crossing of A_{iq} over A_{js} in the diagram $\text{pr}_{xz}(\text{rot}_t(K))$ for some $t \in S_t^1$. Associate to p the ordered *label* $(q_i s_j)$. Then the edges of the graph $\text{TG}(K)$ are labelled. In the case $m = 1$ we miss the indices i, j of components of K and label edges by ordered pairs (qs) , see Figure 3. \blacksquare

For each $t \in S_t^1$, watch the crossings of the diagram $\text{pr}_{xz}(\text{rot}_t(K)) \subset A_{xz} \times \{t\}$, eg the initial diagram $\text{pr}_{xz}(K) \subset A_{xz}$ at $t = 0$ has 3 double crossings, which evolve during the rotation of K . At $t = \pi/4$, the lowest crossing becomes a critical crossing Ψ corresponding to a critical vertex \curvearrowright of $\text{TG}(K)$. At the same $t = \pi/4$ a couple of crossings is born after Reidemeister move II associated to a tangency \curvearrowleft . At $t = \pi/2$ a new crossing is born from a cusp \curvearrowright after Reidemeister move I, which leads to a hanging vertex \curvearrowright of $\text{TG}(K)$. The 2 triple vertices of $\text{TG}(K)$ for $t \in (0, \pi)$ correspond to 2 Reidemeister moves III happening during the rotation of K . A combinatorial explicit construction of the trace graph is in Lemma 6.8.

Theorem 1.4. *Links $K_0, K_1 \subset V$ are isotopic in the solid torus V if and only if their labelled trace graphs $\text{TG}(K_0), \text{TG}(K_1) \subset \mathbb{T}$ can be obtained from each other by an isotopy in \mathbb{T} and a finite sequence of moves in Figure 11.*

Trace graphs of closed braids have combinatorial features, allowing us to recognize them up to all but one type of moves. The following result of [8] is one of very few known polynomial algorithms recognizing topological objects up to isotopy.

Theorem 1.5. *Let $\beta, \beta' \in B_n$ be braids of length $\leq l$. There is an algorithm of complexity $C(n/2)^{n^2/8}(6l)^{n^2-n+1}$ to decide whether $\text{TG}(\hat{\beta})$ and $\text{TG}(\hat{\beta}')$ are related by isotopy in \mathbb{T} and trihedral moves, the constant C does not depend on l and n . In the case of pure braids, the power $n^2/8$ can be replaced by 1. If the closure of a braid is a single curve in the solid torus, then the complexity reduces to $Cn(6l)^{n-1}$.*

1.4. Scheme of proofs.

The *first* double arrow in Figure 4 is a classical reduction of an equivalence of links to extended Reidemeister moves on plane diagrams in Figure 5.

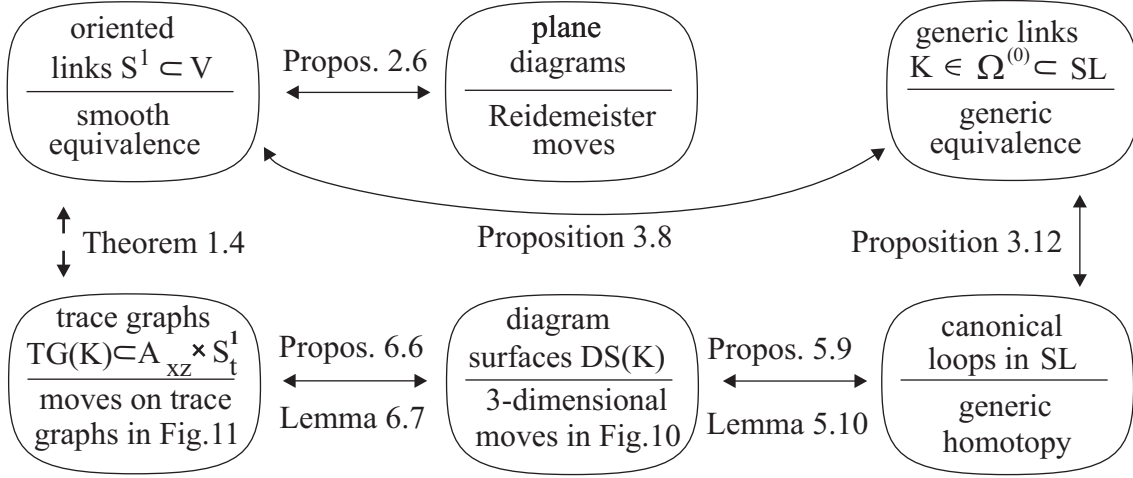


FIGURE 4. A scheme to prove Theorem 1.4.

The *second* arrow is a new reduction to generic links and generic equivalence defined in terms of codimension 1 singularities with respect to the rotation of links in V .

The *third* arrow is a reformulation of the previous reduction in terms of canonical loops of links in the space of all links in the solid torus V .

The *fourth* arrow is a reduction of generic links to their 2-dimensional diagram surfaces considered up to 3-dimensional moves in Figure 10.

The *fifth* arrow is a final reduction of generic links to their trace graphs considered up to equivalence generated by the moves in Figure 11.

The key ingredient of the proofs is a description of versal deformations and bifurcation diagrams of codimension 2 multi local singularities of plane curves in section 4.

Acknowledgements. The second author is especially grateful to Hugh Morton and Farid Tari for fruitful comments and suggestions. He also thanks Yu. Burman, M. Kazaryan, V. Vassiliev, V. Zakalyukin for useful discussions.

2. SINGULAR SUBSPACES IN THE SPACE OF ALL LINKS

2.1. Codimension 1 singularities of link diagrams.

Let M, N be smooth finite dimensional manifolds. Denote by $J_{[l]}^k(M, N)$ the space of all l -tuple k -jets of smooth maps $\xi : M \rightarrow N$ for all tuples $(u_1, \dots, u_l) \in M^l$, see [1, sections I.2]. Let (x_1, \dots, x_m) and (y_1, \dots, y_n) be local coordinates in M and N , respectively. If the map ξ is defined locally by $y_j = \xi_j(x_1, \dots, x_m)$, $j = 1, \dots, n$, then the l -tuple k -jet of the map ξ at a point (u_1, \dots, u_l) is determined by

$$\{x_1, \dots, x_m\}; \quad \{y_1, \dots, y_n\}; \quad \left\{ \frac{\partial \xi_j}{\partial x_i} \right\}; \quad \dots \quad \left\{ \frac{\partial^k \xi_j}{\partial x_{i_1} \dots \partial x_{i_s}} \right\}, \quad i_1 + \dots + i_s = k.$$

The above quantities define local coordinates in $J_{[l]}^k(M, N)$. The l -tuple k -jet $j_{[l]}^k \xi$ of a smooth map $\xi : M \rightarrow N$ can be considered as the map $j_{[l]}^k \xi : M^l \rightarrow J_{[l]}^k(M, N)$, namely (u_1, \dots, u_l) goes to the l -tuple k -jet of the map ξ at (u_1, \dots, u_l) .

Take an open set $W \subset J_{[l]}^k(M, N)$ for some k, l . The set of smooth maps $f : M \rightarrow N$ with l -tuple k -jets from W is called *open*. These sets for all open $W \subset J_{[l]}^k(M, N)$ form a basis of the *Whitney* topology in $C^\infty(M, N)$. So two maps are close in the Whitney topology if they are close with all their derivatives.

Definition 2.1. The space SL of all links $K \subset V$ inherits the *Whitney* topology from $C^\infty(\sqcup_{j=1}^m S_j^1, V)$. A link K defined by a smooth embedding $f : \sqcup_{j=1}^m S_j^1 \rightarrow V$ is called *general* if the diagram $D = \text{pr}_{xz}(K) \subset A_{xz}$ is *general*, namely

- the map $\text{pr}_{xz} \circ f : \sqcup_{j=1}^m S_j^1 \rightarrow A_{xz}$ is a smooth embedding outside finitely many double *crossings*, an overcrossing arc is specified at each crossing;
- the extrema of $\text{pr}_z : D \rightarrow S_z^1$ are not crossings and have distinct z -coordinates.

Denote by $\Sigma^{(0)} \subset \text{SL}$ the subspace of all general links. ■

We consider local singularities, so fix coordinates x, z around each point in A_{xz} . The x -axis is said to be *horizontal*, i.e. it is perpendicular to the vertical core $S_z^1 \subset A_{xz}$. Classical codimension 1 singularities of plane curves were described by David [5, List I on p. 561], namely the ordinary cusp \curlyvee (the A_2 singularity in Arnold's notations), simple tangency \curlyx (A_3) and triple point \curlyx (D_4). The solid torus V has the distinguished vertical direction along S_z^1 , so we also consider singularities with respect to $\text{pr}_z : V \rightarrow S_z^1$, eg Reidemeister move IV is generated by passing through a critical crossing \curlyhook , where one of the tangents is horizontal.

Definition 2.2. A *diagram* D is the image of a smooth map $g : \sqcup_{j=1}^m S_j^1 \rightarrow A_{xz}$.

\curlyx A *triple point* of the diagram D is a transversal intersection p of 3 arcs such that all the tangents at p are not horizontal.

\curlyx A *simple tangency* is an intersection p of 2 arcs given locally by $u = \pm v^2$. We assume that the tangent at p is not horizontal.

\curlyvee An *ordinary cusp* is the singular point p of an arc given locally by $u^2 = v^3$. We assume that the tangent at p is not horizontal.

\curlyhook A *critical crossing* is a transversal intersection p of 2 arcs such that one of the tangents at p is horizontal.

\curvearrowright A *cubical point* is the singular point p of an arc given locally by $z = u^3$, the tangent at p is horizontal.

\curlywedge A *mixed pair* is a pair of a local maximum and a local minimum of the projection $\text{pr}_z : D \rightarrow S_z^1$, lying in the same horizontal line.

\curlywedge An *extreme pair* is a pair of either 2 local maxima or 2 local minima of the projection $\text{pr}_z : D \rightarrow S_z^1$, lying in the same horizontal line.

Given a singularity $\gamma \in \{\curlyx, \curlyx, \curlyvee, \curlyhook, \curvearrowright, \curlywedge, \curlywedge\}$, denote by $\Sigma_\gamma \subset \text{SL}$ the singular subspace consisting of all links $K \subset V$ such that $\text{pr}_{xz}(K)$ is general outside γ .

$$\text{Set} \quad \Sigma^{(1)} = \Sigma_{\curlyx} \cup \Sigma_{\curlyx} \cup \Sigma_{\curlyvee} \cup \Sigma_{\curlyhook} \cup \Sigma_{\curvearrowright} \cup \Sigma_{\curlywedge} \cup \Sigma_{\curlywedge} \subset \text{SL}. \quad \blacksquare$$

2.2. Extended Reidemeister theorem.

Definition 2.3. Let M be a finite dimensional smooth manifold. A subspace $\Lambda \subset M$ is called a *stratified space* if Λ is the union of disjoint smooth submanifolds Λ^i (*strata*) such that the boundary of each stratum is a finite union of strata of less dimensions. Let N be a finite dimensional manifold. A smooth map $\xi : M \rightarrow N$ is *transversal* to a smooth submanifold $U \subset N$ if the spaces $f_*(T_x M)$ and $T_{f(x)} U$ generate $T_{f(x)} N$ for each $x \in M$. A smooth map is $\eta : M \rightarrow N$ *transversal* to a stratified space $\Lambda \subset N$ if the the map η is transversal to each stratum of Λ . ■

Briefly Theorem 2.4 says that any map can be approximated by ‘a nice map’.

Theorem 2.4. (Multi-jet transversality theorem of Thom, see [1, section I.2])
Let M, N be compact smooth manifolds, $\Lambda \subset J_{[l]}^k(M, N)$ be a stratified space. Given a smooth map $\xi : M \rightarrow N$ there is a smooth map $\eta : M \rightarrow N$ such that

- *the map η is arbitrarily close to ξ with respect to the Whitney topology;*
- *the l -tuple k -jet $j_{[l]}^k \eta : M^l \rightarrow J_{[l]}^k(M, N)$ is transversal to $\Lambda \subset J_{[l]}^k(M, N)$.* □

Lemma 2.5. (a) *The subspace $\Sigma^{(1)}$ has codimension 1 in the space SL.*

(b) *The subspace $\Sigma^{(0)}$ is open and dense in the space SL.*

Sketch. (a) It is a standard computation in the space $J_{[3]}^1(\mathbb{R}, \mathbb{R}^2)$ of 3-tuple 1-jets of maps $(x(r), z(r)) : \mathbb{R} \rightarrow \mathbb{R}^2$. For instance, fixing 3 parameters r_1, r_2, r_3 , the subspace Σ_{\times} maps to the subspace of $J_{[3]}^1(\mathbb{R}, \mathbb{R}^2)$ given by 4 equations $x(r_1) = x(r_2) = x(r_3)$, $z(r_1) = z(r_2) = z(r_3)$ and 3 inequalities $\dot{z}(r_i) \neq 0$, $i = 1, 2, 3$, meaning that the tangents are not horizontal, hence the codimension of the subspace $\Sigma_{\times} \subset \text{SL}$ is 1 after forgetting the 3 parameters. Analogously Σ_{γ} maps to the subspace given by 4 equations $\dot{x}(r_1) = \dot{z}(r_1) = 0$, $r_1 = r_2 = r_3$, hence the codimension of $\Sigma_{\gamma} \subset \text{SL}$ is 1. A similar detailed argument will be given in the proof of Lemma 3.5.

(b) The conditions of Definition 2.1 define an open subset of SL whose complement is clearly the closure of the codimension 1 subspace $\Sigma^{(1)}$ from Definition 2.2. □

The following result immediately follows from Lemma 2.5 since by Theorem 2.4 any isotopy in the space SL of links can be approximated by a path transversally intersecting the singular subspace $\Sigma^{(1)} \subset \text{SL}$ of codimension 1.

Proposition 2.6. *Any smooth link can be approximated by a general link. General links are isotopic if and only if their diagrams can be obtained from each other by a plane isotopy and finitely many Reidemeister moves in Figure 5.* □

In Figure 5 orientations of arcs and symmetric images of the moves are omitted.

2.3. The co-orientation of codimension 1 subspaces.

Using Gauss diagrams of link diagrams, we define the co-orientation of codimension 1 subspaces $\Sigma_{\times}, \Sigma_{\gamma}, \Sigma_{\gamma}, \Sigma_{\cap}$ from Definition 2.2.

Definition 2.7. Let a general link K be defined by $f : \sqcup_{j=1}^m S_j^1 \rightarrow V$. The *Gauss diagram* $\text{GD}(K)$ is the union $\sqcup_{j=1}^m S_j^1$ with chords connecting points s_1, s_2 such that $\text{pr}_{xz}(f(s_1)) = \text{pr}_{xz}(f(s_2))$. Gauss diagrams GD_1, GD_2 are *equivalent* if there is an orientation preserving diffeomorphism of $\sqcup_{j=1}^m S_j^1$ such that the endpoints of any chord of GD_1 map onto the endpoints of a chord of GD_2 and vice versa. ■

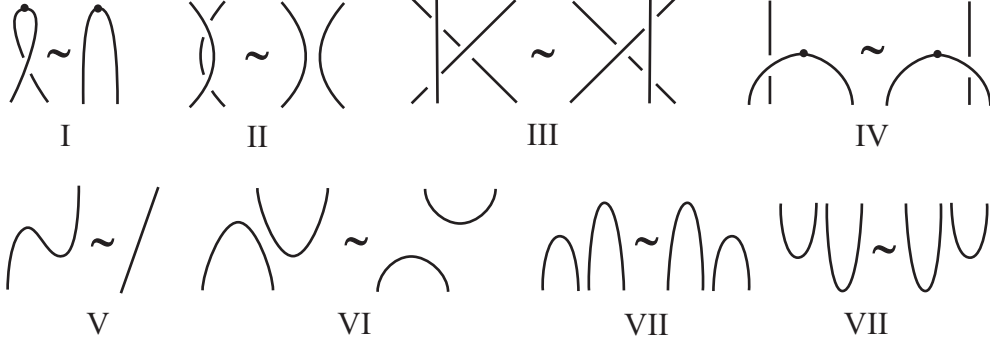


FIGURE 5. Reidemeister moves taking into account local extrema

Definition 2.8. For each of 2 types of oriented triple points, the *co-orientation* of Σ_{\times} is defined in terms of the Gauss diagrams of the corresponding links K_{\pm} in Figure 6. Assume that, while $t \in S_t^1$ increases, the point $\text{rot}_t(K) \in \text{SL}$ passes through Σ_{\times} from the negative side to the positive one. Then associate to the corresponding triple vertex of $\text{TG}(K)$ the *positive* sign $+$, otherwise take the *negative* sign $-$. The *co-orientations* of Σ_{χ} , Σ_{γ} , Σ_{\hookrightarrow} are similarly defined in Figure 6. ■

Look at the trefoil K in Figure 2 and its trace graph $\text{TG}(K)$ in Figure 3. Consider the first triple vertex of $\text{TG}(K)$ at the critical moment $t_1 \in (\pi/4, \pi/2)$. The knot $\text{rot}_{\pi/4}(K)$ is on the positive side of Σ_{\times} (the 1st type in Figure 6), while $\text{rot}_{\pi/2}(K)$ is on the negative side of Σ_{\times} , ie the first triple vertex has the positive sign. At the second triple vertex for $t_2 \in (\pi/2, 3\pi/4)$, the knot $\text{rot}_t(K)$ goes from the negative side to the positive side. So the second triple point also the positive sign.

3. GENERIC LINKS, EQUIVALENCES, LOOPS AND HOMOTOPIES

3.1. The canonical loop of a link and generic links.

Generic links will be defined as the most generic points in the space SL of all links $K \subset V$ with respect to the rotation rot_t of the solid torus V .

Definition 3.1. The *canonical loop* $\text{CL}(K) \subset \text{SL}$ of a smooth link $K \subset V$ is the union of the rotated links $\text{rot}_t(K) \in \text{SL}$ over all $t \in S_t^1$.

A link $K \subset V$ is *generic* if there are finitely many $t_1, \dots, t_k \in S_t^1$ such that

- for all $t \notin \{t_1, \dots, t_k\}$, the links $\text{rot}_t(K)$ are general, ie $\text{rot}_t(K) \in \Sigma^{(0)}$;
- $\text{CL}(K)$ transversally intersects $\Sigma_{\times} \cup \Sigma_{\chi} \cup \Sigma_{\gamma} \cup \Sigma_{\hookrightarrow}$ at each $t \in \{t_1, \dots, t_k\}$.

Denote by $\Omega^{(0)} \subset \text{SL}$ the subspace of all generic links in V . ■

Morse modifications of index 1 would change the trace graph dramatically. Luckily following Lemma 3.2 shows that they can not occur under strong equivalence. More exactly Lemma 3.2 shows that the canonical loop $\text{CL}(K)$ never touches the subspace $\Sigma_{\chi} \cup \Sigma_{\gamma} \cup \Sigma_{\hookrightarrow}$ for any link K . Therefore the transversality from the last condition of Definition 3.1 is relevant only for the subspace Σ_{\times} .

Lemma 3.2. (Main topological lemma) *For any link $K \subset V$, the canonical loop $\text{CL}(K)$ does not touch the subspace $\Sigma_{\chi} \cup \Sigma_{\gamma} \cup \Sigma_{\hookrightarrow}$. More formally, if $K \in \Sigma_{\gamma}$ for $\gamma = \chi, \gamma, \hookrightarrow$, the links $\text{rot}_{\pm\varepsilon}(K)$ are on different sides of Σ_{γ} for small $\varepsilon > 0$.*

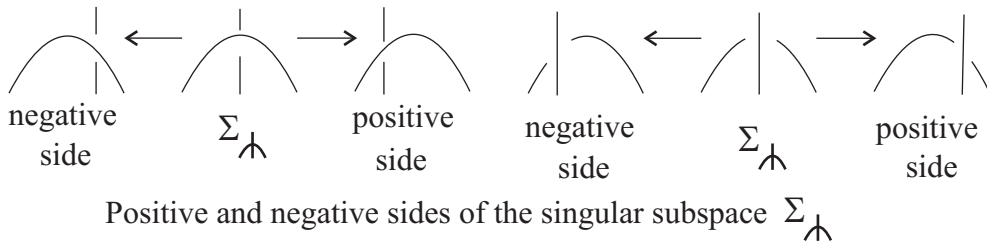
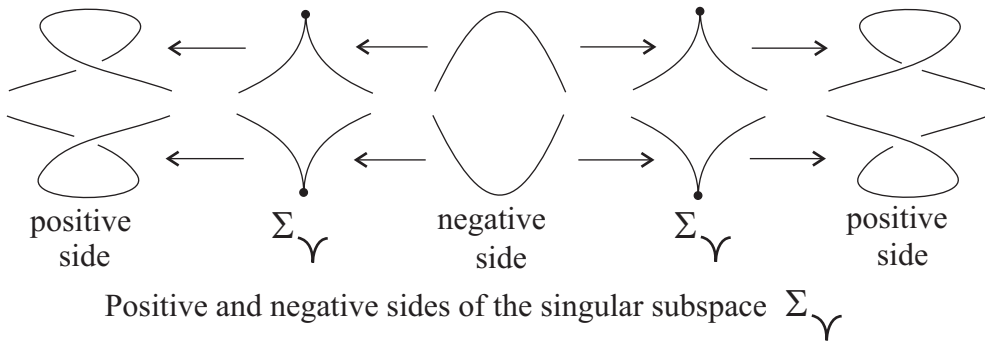
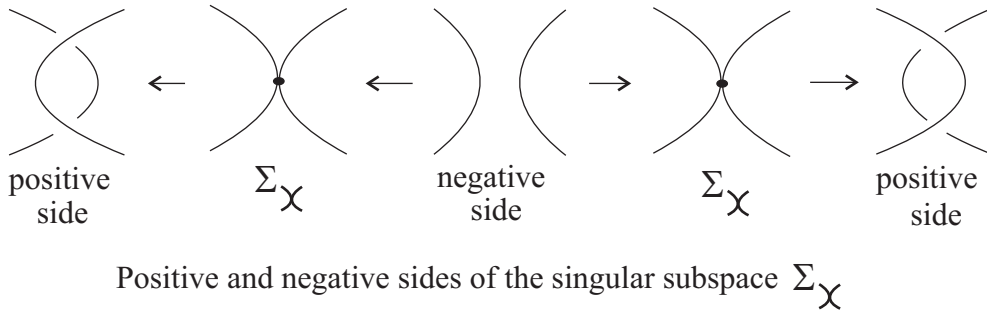
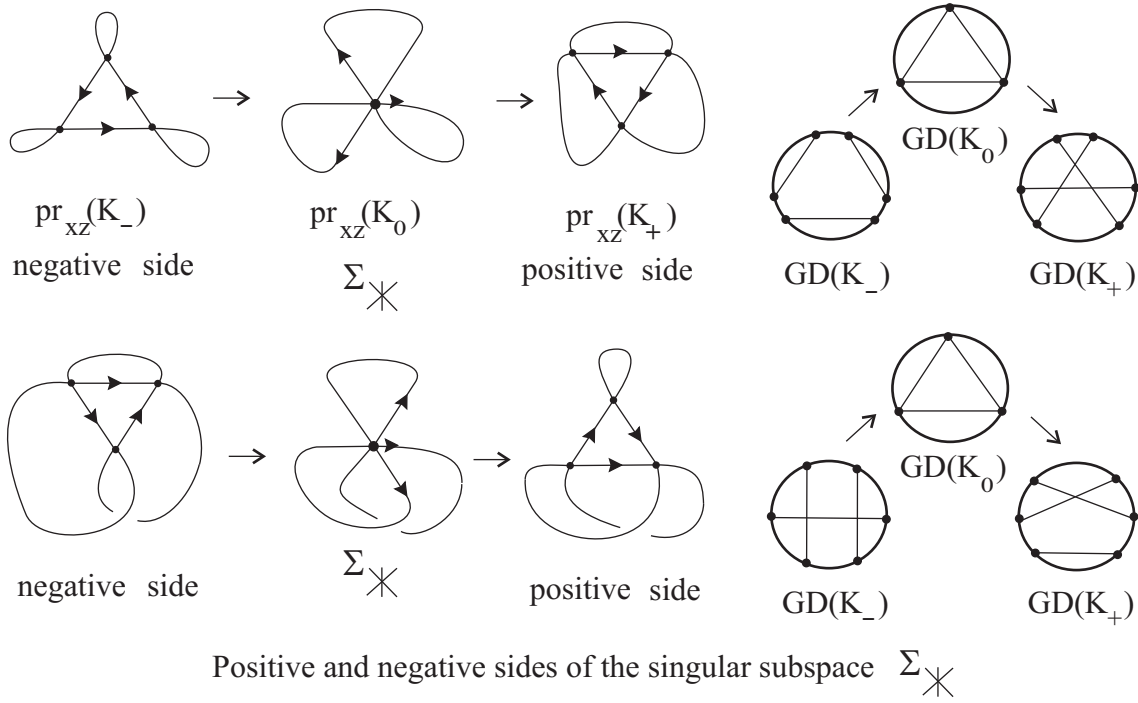


FIGURE 6. How to define the co-orientations of codimension 1 subspaces

Proof. For the subspaces Σ_{χ} and Σ_{γ} , the projections of two small arcs with a tangent point (respectively, a cusp) are interchanged under the rotation.

Figure 6 shows that the links $\text{rot}_{\pm\epsilon}(K)$ are on different sides of Σ_{χ} and Σ_{γ} , respectively, since the tangent at p is not horizontal, ie not orthogonal to the vertical axis S_z^1 . The argument for $\Sigma_{\mathfrak{h}}$ is the same, since one tangent at the critical crossing is not horizontal, see the last picture of Figure 6. \square

Example 3.3. The canonical loop $\text{CL}(K)$ of a knot $K \subset V$ can touch the subspace $\Sigma_{\mathfrak{X}}$. Consider the three arcs $J_1, J_2, J_3 \subset \mathbb{R}^3$ defined by (see Figure 7 below)

$$\begin{cases} x_1 = \tau u^2, \\ y_1 = 0, \\ z_1 = u; \end{cases} \quad \begin{cases} x_2 = u, \\ y_2 = -1, \\ z_2 = u; \end{cases} \quad \begin{cases} x_3 = -u, \\ y_3 = 1, \\ z_3 = u; \end{cases} \quad u \in \mathbb{R}, \tau > 0.$$

Under the composition $\text{pr}_{xz} \circ \text{rot}_t$, the arcs J_1, J_2, J_3 map to the following ones:

$$x_1(t) = \tau z_1^2 \cos t, \quad x_2(t) = z_2 \cos t + \sin t, \quad x_3(t) = -z_3 \cos t - \sin t,$$

where z_1, z_2, z_3 are constants. For small $t = \epsilon > 0$, the double crossing $p_{23} = \text{pr}_{xz}(\text{rot}_\epsilon(J_2)) \cap \text{pr}_{xz}(\text{rot}_\epsilon(J_3))$ has the coordinates $x = 0, z = -\tan \epsilon$. Then p_{23} is at the left of the first rotated arc $x_1(t) = \tau z_1^2 \cos t$ with respect to X .

For $t = -\epsilon < 0$, the crossing with $x = 0, z = \tan \epsilon$ is also at the left of the first arc. Take a knot $K \in \Sigma_{\mathfrak{X}}$ containing small parts of the arcs described above. Then $\text{rot}_{\pm\epsilon}(K)$ are on the same side of $\Sigma_{\mathfrak{X}}$. This means that, under the rotation of K , Reidemeister move III is not performed for the diagram $\text{pr}_{xz}(\text{rot}_t(K))$.

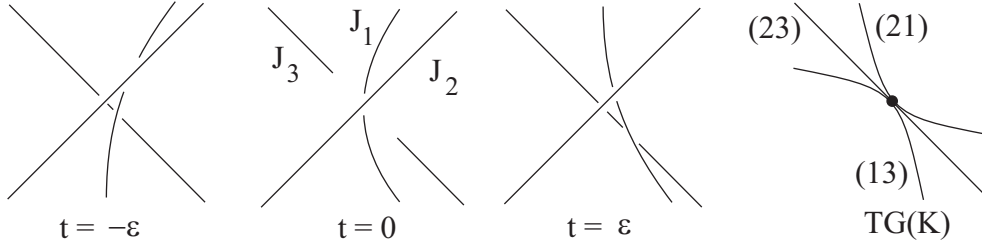


FIGURE 7. $\text{CL}(K)$ may touch the subspace of triple points.

3.2. Codimension 2 singularities and generic equivalences.

Classical codimension 2 singularities of plane curves were described by David [5, List II on p. 561], namely the rumpoidal cusp \mathfrak{N} (the A_4 singularity in Arnold's notations), intersected cusp \mathfrak{Y} (D_5), tangent triple point \mathfrak{X} (D_4), cubic tangency \mathfrak{J} (A_5) and ordinary quadruple point \mathfrak{X} (X_9). We need to distinguish more refined singularities since the canonical loop of a link may not be transversal to some singular subspace, eg it is transversal to the codimension 2 subspace of horizontal cusps $\Sigma_{\mathfrak{N}}$, but not to the codimension 1 subspace of all cusps $\Sigma_{\mathfrak{Y}} \cup \Sigma_{\mathfrak{N}}$. All tangents below are not *horizontal* unless stated otherwise.

Definition 3.4. (*codimension 2 singularities of link diagrams*)

Let D be a diagram, ie the image of a smooth map $g : \sqcup_{j=1}^m S_j^1 \rightarrow A_{xz}$.

\mathfrak{X} A *quadruple point* of D is a transversal intersection p of 4 arcs.

- \times A *tangent triple point* of D is an intersection p of 3 arcs, the first two arcs have a simple tangency and do not touch the third arc.
- \succ An *intersected cusp* of D is an intersection of 2 arcs, where the first arc has an ordinary cusp whose vector (\ddot{x}, \ddot{z}) does not touch the second arc.
- \lrcorner A *cubic tangency* is an intersection of 2 arcs given locally by $u = 0, u = v^3$.
- \rhd A *ramphoidal cusp* is the singular point of an arc, given locally by $u^2 = v^5$.
- \neg A *horizontal cusp* is an ordinary cusp with horizontal tangent.
- \times A *mixed tangency* is a simple tangency with a horizontal tangent such that one of the extrema is a maximum, another one is a minimum.
- \cap An *extreme tangency* is a simple tangency with a horizontal tangent such that **both** extrema are either maxima or minima.
- $\times, \text{ (with horizontal tangent) }$ A *horizontal triple point* is a triple intersection, where the tangent line of the first arc is horizontal, the tangent lines of the other arcs are not horizontal.

Given a singularity $\delta \in \{*, \times, \succ, \lrcorner, \rhd, \times, \text{ (with horizontal tangent) }, \neg, \times, \cap\}$, denote by Σ_δ the union of all links $K \subset V$ such that the diagram $\text{pr}_{xz}(K)$ is general outside δ . Set

$$\Sigma^{(2)} = \Sigma_* \cup \Sigma_\times \cup \Sigma_\succ \cup \Sigma_{\lrcorner} \cup \Sigma_{\rhd} \cup \Sigma_{\times} \cup \Sigma_{\text{ (with horizontal tangent) }} \cup \Sigma_\neg \cup \Sigma_{\times} \cup \Sigma_{\cap} \subset \text{SL}. \quad \blacksquare$$

Lemma 3.5. *The singular subspace $\Sigma^{(2)}$ has codimension 2 in the space SL.*

Proof. We use multi jets of maps $(x(r), z(r)) : \mathbb{R} \rightarrow \mathbb{R}^2$ defining a diagram D . Fixing 4 points r_1, r_2, r_3, r_4 , each singularity δ from Definition 3.4 can be described in terms of 4-tuple 3-jets from the space $J_{[4]}^3(\mathbb{R}, \mathbb{R}^2)$, where each point has the 36 coordinates:

$$J_{[4]}^3(\mathbb{R}, \mathbb{R}^2) : \quad \left\{ \begin{array}{llll} r_i; & x(r_i), & z(r_i); & \dot{x}(r_i), \quad \dot{z}(r_i); \\ & \ddot{x}(r_i), & \ddot{z}(r_i); & \ddot{x}(r_i), \quad \ddot{z}(r_i); \end{array} \quad i = 1, 2, 3, 4. \right.$$

The jets over all $K \in \Omega_\delta$ form the finite dimensional *subspace* $\tilde{\Sigma}_\delta \subset J_{[4]}^3(\mathbb{R}, \mathbb{R}^2)$.

A simple tangency of 2 arcs at r_i, r_j is described by $\Gamma_{ij} = \begin{vmatrix} \dot{x}(r_i) & \dot{x}(r_j) \\ \dot{z}(r_i) & \dot{z}(r_j) \end{vmatrix} = 0$. The frequent inequality $\dot{z}(r_i) \neq 0$ below says that the tangent of D at r_i is not horizontal. The string $r_1 \neq r_2 \neq r_3 \neq r_4$ will mean that r_1, r_2, r_3, r_4 are pairwise disjoint.

$$\begin{aligned} \tilde{\Sigma}_* & \left\{ \begin{array}{l} x(r_1) = x(r_2) = x(r_3) = x(r_4), \quad r_1 \neq r_2 \neq r_3 \neq r_4, \\ z(r_1) = z(r_2) = z(r_3) = z(r_4), \quad \dot{z}(r_i) \neq 0, \Gamma_{ij} \neq 0, i \neq j; \end{array} \right. \\ \tilde{\Sigma}_\times & \left\{ \begin{array}{l} x(r_1) = x(r_2) = x(r_3), \quad r_1 \neq r_2 \neq r_3 = r_4, \dot{z}(r_i) \neq 0, \\ z(r_1) = z(r_2) = z(r_3), \quad \Gamma_{12} = 0, \Gamma_{23} \neq 0, \Gamma_{13} \neq 0; \end{array} \right. \\ \tilde{\Sigma}_\succ & \left\{ \begin{array}{l} x(r_1) = x(r_2), z(r_1) = z(r_2), \quad \ddot{z}(r_1) \neq 0, \dot{z}(r_2) \neq 0, \left| \begin{vmatrix} \ddot{x}(r_1) & \dot{x}(r_2) \\ \ddot{z}(r_1) & \dot{z}(r_2) \end{vmatrix} \right| \neq 0; \\ \dot{x}(r_1) = \dot{z}(r_1) = 0, \quad r_1 \neq r_2 = r_3 = r_4, \end{array} \right. \\ \tilde{\Sigma}_{\lrcorner} & \left\{ \begin{array}{l} x(r_1) = x(r_2), z(r_1) = z(r_2), \quad \left| \begin{vmatrix} \ddot{x}(r_1) & \dot{x}(r_2) \\ \ddot{z}(r_1) & \dot{z}(r_2) \end{vmatrix} \right| = 0, \left| \begin{vmatrix} \ddot{x}(r_1) & \dot{x}(r_2) \\ \ddot{z}(r_1) & \dot{z}(r_2) \end{vmatrix} \right| \neq 0; \\ r_1 \neq r_2 = r_3 = r_4, \Gamma_{12} = 0, \\ \dot{z}(r_1) \neq 0, \quad \dot{z}(r_2) \neq 0, \end{array} \right. \\ \tilde{\Sigma}_{\rhd} & \left\{ \begin{array}{l} \dot{x}(r_1) = \dot{z}(r_1) = 0, \quad \ddot{z}(r_1) \neq 0 \quad \left| \begin{vmatrix} \ddot{x}(r_1) & \ddot{x}(r_1) \\ \ddot{z}(r_1) & \ddot{z}(r_1) \end{vmatrix} \right| = 0; \\ r_1 = r_2 = r_3 = r_4, \end{array} \right. \end{aligned}$$

Points $f(r_i), f(r_j), f(r_k) \in K$ project to the same point under $\text{pr}_{xz} : \text{rot}_t(K) \rightarrow \mathbb{A}_{xz} \times \{t\}$ for some t if and only if $z(r_i) = z(r_j) = z(r_k)$, $\begin{vmatrix} \Delta x_{ij} & \Delta x_{jk} \\ \Delta y_{ij} & \Delta y_{jk} \end{vmatrix} = 0$. The last determinant is (up to the sign) the area of the triangle with the vertices $(x(r_i), y(r_i)), (x(r_j), y(r_j)), (x(r_k), y(r_k))$ in the horizontal plane $\{z(r_i) = z(r_j) = z(r_k)\}$.

Set $\Delta_{ij} = \begin{vmatrix} \dot{x}(r_i) & \dot{x}(r_j) & \Delta x_{ij} \\ \dot{y}(r_i) & \dot{y}(r_j) & \Delta y_{ij} \\ \dot{z}(r_i) & \dot{z}(r_j) & \Delta z_{ij} \end{vmatrix}$. The diagram $\text{pr}_{xz}(\text{rot}_t(K))$ contains two arcs having a simple tangency at $r = r_i, r = r_j$ and some t if and only if $z(r_i) = z(r_j)$ and $\Delta_{ij} = 0$, ie the straight line through $f(r_i), f(r_j) \in K$ lies in the plane spanned by the tangent vectors of K at $r = r_i$ and $r = r_j$.

We describe analytically the subspaces $\tilde{\Omega}_\delta$ associated to the singularities

$$*, \times, \succ, \mathcal{J}, \curvearrowright, \bowtie, \text{X}, \curvearrowleft, \curvearrowright, \curvearrowleft, \curvearrowright, \overline{\text{X}}.$$

$$\begin{aligned} \tilde{\Omega}_* & \left\{ \begin{array}{l} z(r_1) = z(r_2) = z(r_3) = z(r_4), \\ r_1 \neq r_2 \neq r_3 \neq r_4, \\ \dot{z}(r_i) \neq 0, \ i = 1, 2, 3, 4, \end{array} \quad \begin{vmatrix} \Delta x_{12} & \Delta x_{23} \\ \Delta y_{12} & \Delta y_{23} \end{vmatrix} = \begin{vmatrix} \Delta x_{12} & \Delta x_{24} \\ \Delta y_{12} & \Delta y_{24} \end{vmatrix} = 0, \right. \\ & \quad \Delta_{ij} \neq 0, \ i, j \in \{1, 2, 3, 4\}, \ i \neq j; \\ \tilde{\Omega}_\times & \left\{ \begin{array}{l} z(r_1) = z(r_2) = z(r_3), \\ r_1 \neq r_2 \neq r_3 = r_4, \\ \dot{z}(r_i) \neq 0, \ i = 1, 2, 3, \end{array} \quad \begin{vmatrix} \Delta x_{12} & \Delta x_{23} \\ \Delta y_{12} & \Delta y_{23} \end{vmatrix} = 0, \right. \\ & \quad \Delta_{12} = 0, \ \Delta_{23} \neq 0, \ \Delta_{13} \neq 0; \\ \tilde{\Omega}_\succ & \left\{ \begin{array}{l} z(r_1) = z(r_2), \\ \dot{z}(r_1) = 0, \ \ddot{z}(r_1) \neq 0, \\ \dot{z}(r_2) \neq 0, \end{array} \quad \begin{vmatrix} \dot{x}(r_1) & \dot{x}(r_2) \\ \dot{y}(r_1) & \dot{y}(r_2) \end{vmatrix} = 0, \quad \begin{vmatrix} \ddot{x}(r_1) & \ddot{x}(r_2) & \Delta x_{12} \\ \ddot{y}(r_1) & \ddot{y}(r_2) & \Delta y_{12} \\ \ddot{z}(r_1) & \ddot{z}(r_2) & \Delta z_{12} \end{vmatrix} \neq 0; \right. \\ & \quad r_1 \neq r_2 = r_3 = r_4, \\ \tilde{\Omega}_{\mathcal{J}} & \left\{ \begin{array}{l} z(r_1) = z(r_2), \quad \Delta_{12} = 0, \\ r_1 \neq r_2 = r_3 = r_4, \\ \dot{z}(r_1) \neq 0, \quad \dot{z}(r_2) \neq 0, \end{array} \quad \begin{vmatrix} \ddot{x}(r_1) & \ddot{x}(r_2) & \Delta x_{12} \\ \ddot{y}(r_1) & \ddot{y}(r_2) & \Delta y_{12} \\ \ddot{z}(r_1) & \ddot{z}(r_2) & \Delta z_{12} \end{vmatrix} = 0; \right. \\ \tilde{\Omega}_{\curvearrowright} & \left\{ \begin{array}{l} \dot{z}(r_1) = 0, \quad \ddot{z}(r_1) \neq 0, \\ r_1 = r_2 = r_3 = r_4, \end{array} \quad \frac{\ddot{x}(r_1)}{\ddot{x}(r_1)} = \frac{\ddot{y}(r_1)}{\ddot{y}(r_1)} = \frac{\ddot{z}(r_1)}{\ddot{z}(r_1)}. \right. \end{aligned}$$

The last equations with 3 fractions mean that the vectors of the 2nd and 3rd derivatives are collinear, which corresponds to the similar condition for $\tilde{\Sigma}_{\curvearrowright}$ in the proof of Lemma 3.5. If a denominator is zero, the numerator must be also zero.

$$\begin{aligned} \tilde{\Omega}_{\bowtie} \cup \tilde{\Omega}_{\text{X}} & \left\{ \begin{array}{l} z(r_1) = z(r_2) = z(r_3), \quad r_1 \neq r_2 \neq r_3 = r_4, \\ \dot{z}(r_1) = 0, \ \ddot{z}(r_1) \neq 0, \ \dot{z}(r_2) \neq 0, \ \dot{z}(r_3) \neq 0, \end{array} \quad \begin{vmatrix} \Delta x_{12} & \Delta x_{23} \\ \Delta y_{12} & \Delta y_{23} \end{vmatrix} = 0; \right. \\ \tilde{\Omega}_{\curvearrowleft} & \left\{ \begin{array}{l} \dot{z}(r_1) = \ddot{z}(r_1) = 0, \quad r_1 = r_2 = r_3 = r_4, \quad \ddot{z}(r_1) \neq 0; \end{array} \right. \\ \tilde{\Omega}_{\curvearrowright} \cup \tilde{\Omega}_{\curvearrowleft} & \left\{ \begin{array}{l} z(r_1) = z(r_2), \quad r_1 \neq r_2 = r_3 = r_4, \\ \dot{z}(r_1) = \dot{z}(r_2) = 0, \quad \ddot{z}(r_1) \neq 0, \ \ddot{z}(r_2) \neq 0. \end{array} \right. \end{aligned}$$

If $\dot{z}(r_i) \neq 0$, then locally r_i can be considered as a function of z , hence any function of (several) r_i can be differentiated with respect to z . Below the tangency with Σ_{\bowtie} means that the derivative of the vanishing determinant $\Delta = \begin{vmatrix} \Delta x_{12} & \Delta x_{23} \\ \Delta y_{12} & \Delta y_{23} \end{vmatrix}$ defining a triple point under the projection $\text{pr}_{xz} : \text{rot}_t(K) \rightarrow \mathbb{A}_{xz} \times \{t\}$ also vanishes.

$$\tilde{\Omega}_{\overline{\times}} \left\{ \begin{array}{l} z(r_1) = z(r_2) = z(r_3), \quad r_1 \neq r_2 \neq r_3 = r_4 \quad \Delta_{ij} \neq 0, \\ \Delta = \frac{d}{dz}\Delta = 0, \quad \frac{d^2}{dz^2}\Delta \neq 0, \quad \Delta = \begin{vmatrix} \Delta x_{12} & \Delta x_{23} \\ \Delta y_{12} & \Delta y_{23} \end{vmatrix} \quad \begin{array}{l} i \neq j, \\ \dot{z}(r_i) \neq 0. \end{array} \end{array} \right.$$

Generic inequalities $\frac{dg}{dz} \neq 0$ should be added to the descriptions above for each condition $g = 0$, which guarantees no tangency of the canonical loop with the corresponding subspace Σ_δ . In important cases like $\tilde{\Omega}_{\searrow}$ we explicitly accompanied $\dot{z}(r_1) = 0$ with $\ddot{z}(r_2) \neq 0$ equivalent to $\frac{\dot{z}(r_1(z))}{dz} \neq 0$, but also every equation like $z(r_1) = z(r_2)$ should be accompanied with $\frac{dz(r_1(z))}{dz} \neq \frac{dz(r_2(z))}{dz}$.

Each subspace $\tilde{\Omega}_\delta$ is defined by 5 equations, hence $\text{codim } \tilde{\Omega}_\delta = 5$ in $J_{[4]}^3(\mathbb{R}, \mathbb{R}^3)$. The subspaces Ω_δ introduced geometrically in Definition 3.6 correspond to $\tilde{\Omega}_\delta$ by adding 4 points r_1, r_2, r_3, r_4 on a link. When we forget about these points the codimension decreases by 4, ie $\text{codim } \Omega_\delta = 1$ in the space SL of all links $K \subset V$.

(b) The conditions of Definition 3.6 define an open subset of SL whose complement is clearly the closure of the codimension 1 subspace $\Omega^{(1)}$. \square

The following result similar to Proposition 2.6 follows from Lemma 3.7 since by Theorem 2.4 any isotopy in the space SL of links can be approximated by a path transversally intersecting the singular subspace $\Omega^{(1)} \subset \text{SL}$.

Proposition 3.8. (a) *Any smooth link can be approximated by a generic link.*

(b) *Any smooth equivalence of links can be approximated by a generic one.* \square

3.3. Generic loops and generic homotopies in the space of links.

A loop of links $\{K_t\} \subset \text{SL}$ means a *smooth* loop, ie a smooth map $S_t^1 \rightarrow \text{SL}$. Generic loops provide a suitable generalization of the canonical loop.

Definition 3.9. A smooth loop of links $\{K_t\} \subset \text{SL}$, $t \in S_t^1$, is called *generic* if there are finitely many critical moments $t_1, \dots, t_k \in S_t^1$ such that

- the link K_t maps to $K_{t+\pi}$ under the rotation through π for every $t \in S_t^1$;
- for all $t \notin \{t_1, \dots, t_k\}$, the links K_t are general, ie $K_t \in \Sigma^{(0)}$;
- $\{K_t\}$ transversally intersects $\Sigma_{\times} \cup \Sigma_{\searrow} \cup \Sigma_{\gamma} \cup \Sigma_{\wedge}$ at each $t = t_1, \dots, t_k$. \blacksquare

Due to Lemmas 2.5, 3.7 any loop can be approximated by a generic loop. But a generic loop may be too trivial. For instance, a loop $S_t^1 \rightarrow \text{SL}$ contractible to a generic link through generic links carries information about only one diagram. More interesting objects are generic loops homotopic to canonical loops.

Definition 3.10. A smooth family $\{L_s\}$ of loops, $s \in [0, 1]$, is called a *generic* homotopy if there are finitely many critical moments $s_1, \dots, s_k \in [0, 1]$ such that

- for $s \notin \{s_1, \dots, s_k\}$, the loop L_s is generic in the sense of Definition 3.9;
- for each $s \in \{s_1, \dots, s_k\}$, the loop L_s fails to be generic since either L_s transversally intersects $\Sigma^{(2)}$ or L_s touches Σ_{\times} at exactly one point. \blacksquare

- Lemma 3.11.** (a) *The canonical loop of any generic link is a generic loop.*
 (b) *Any generic equivalence $\{K_s\}$, $s \in [0, 1]$, of links provides the generic homotopy of loops $\{\text{CL}(K_s)\}$ of links.*
 (c) *If canonical loops $\text{CL}(K_0)$ and $\text{CL}(K_1)$ of generic links K_0 and K_1 are generically homotopic then K_0 and K_1 are generically equivalent.*

Proof. (a) The canonical loop of any link is symmetric in the sense that $\text{rot}_t(K)$ maps to $\text{rot}_{t+\pi}(K)$ under the rotation through π for every $t \in S_t^1$. The other conditions of Definition 3.9 correspond to the conditions of Definition 3.1.

(b) Compare Definition 3.6 with Definitions 3.9 and 3.10.

(c) Let $\{L_s\}$, $s \in [0, 1]$, be a generic homotopy between $\text{CL}(K_0)$ and $\text{CL}(K_1)$. The loops L_s can be represented by a cylinder $S_t^1 \times [0, 1]$ mapped to the space SL . Take a smooth path connecting K_0 and K_1 inside the cylinder. This smooth equivalence can be approximated by a generic one due to Proposition 3.8b. \square

By Lemma 3.11 the classification of links reduces to their canonical loops.

Proposition 3.12. *Generic links are generically equivalent in V if and only if their canonical loops are generically homotopic in the space SL of all links $K \subset V$.* \square

4. THROUGH CODIMENSION 2 SINGULARITIES

4.1. Versal deformations of codimension 2 singularities.

To understand what happens when the canonical loop of a link passes through the singular subspace $\Sigma^{(2)}$, we study bifurcation diagrams of codimension 2 singularities.

Lemma 4.1. *The codimension 2 singularities from Definition 3.4 have the normal forms in the table below, where r is the parameter on the curve and*

- \mathcal{A}_e is the extended right-left equivalence, i.e. diffeomorphisms of \mathbb{R}^2 don't fix 0;
- \mathcal{A}_z is the restricted right-left equivalence such that left diffeomorphisms of \mathbb{R}^2 have the form $(g(x, z), h(z))$, where $g(x, z) : \mathbb{R}^2 \rightarrow \mathbb{R}$, $h(z) : \mathbb{R} \rightarrow \mathbb{R}$ are diffeomorphisms.

\ast, \mathcal{A}_e	$\{x = 0, z = r\}, \{x = r, z = r\}, \{x = -r, z = r\}, \{x = er, z = r\}$
$\mathcal{X}, \mathcal{A}_e$	$\{x = r^2, z = r\}, \{x = 0, z = r\}, \{x = r, z = r\}$
$\mathcal{Y}, \mathcal{A}_e$	$\{x = r^3, z = r^2\}, \{x = r, z = r\}$
$\mathcal{J}, \mathcal{A}_e$	$\{x = r^3, z = r\}, \{x = 0, z = r\}$
$\mathcal{N}, \mathcal{A}_e$	$\{x = r^5, z = r^2\}$
\neg, \mathcal{A}_z	$\{x = r^2, z = r^3\}$
$\mathcal{X}, \mathcal{A}_z$	$\{x = r, z = r^2\}, \{x = r, z = -r^2\}$
$\mathcal{M}, \mathcal{A}_z$	$\{x = r, z = -2r^2\}, \{x = r, z = -r^2\}$
$\mathcal{K}, \mathcal{A}_z$	$\{x = r, z = -r^2\}, \{x = r, z = r\}, \{x = -r, z = r\}$
$\mathcal{K}, \mathcal{A}_z$	$\{x = r, z = -r^2\}, \{x = r, z = r\}, \{x = 2r, z = r\}$

Sketch. The normal forms up to \mathcal{A}_e -equivalence are classical, eg the parameter $e \neq 0$ in the normal form of \ast (X_9) can not be skipped as the cross-ratio of 4 slopes is invariant under diffeomorphisms, see [14, Lemma 6.5]. The singularities \mathcal{X} , \neg , \mathcal{M} , \mathcal{K} , \mathcal{K} should be considered up to \mathcal{A}_z -equivalence respecting $\{z = \text{const}\}$,

otherwise they don't have codimension 2, e.g. the normal form (r^2, r^3) of \prec is not \mathcal{A}_z -equivalent to the normal form (r^3, r^2) of \succ . Deducing new normal forms is similar, eg the horizontal cusp \prec is defined by the conditions $\dot{x}(0) = \dot{z}(0) = \ddot{z}(0) = 0$, hence $x(r) = ar^2 + \dots$, $z(r) = br^3 + \dots$, which normalises to (r^2, r^3) as required. \square

Mancini and Ruas [12] have shown that the group \mathcal{A}_z from Lemma 4.1 is geometric in the sense of Damon [4]. So the standard technique of singularity theory can be applied to find versal deformations of corresponding codimension 2 singularities.

We consider horizontal triple points \bowtie and \bowtie separately, because the associated moves on trace graphs look slightly different in Figure 11ix, 11x. A deformation of a germ $(x(r), z(r)) : \mathbb{R} \rightarrow \mathbb{R}^2$ with parameters a, b is a germ $F : \mathbb{R} \times \mathbb{R}^2 \rightarrow \mathbb{R}^2$ such that $F(r; 0, 0) \equiv (x(r), z(r))$. A deformation F is *versal* if any other deformation can be obtained from F by actions of the corresponding group \mathcal{A}_e or \mathcal{A}_z .

The versality can be checked using the following tangent spaces at germs in the space of deformations. Let T^r be the *right* tangent space at a germ $(x(r), z(r))$ generated by the right diffeomorphisms $\mathbb{R} \rightarrow \mathbb{R}$, eg the right space T^r at (r^5, r^2) of \bowtie consists of $(5r^4 f(r), 2r f(r))$, where $f : \mathbb{R} \rightarrow \mathbb{R}$. Denote by T^l the *left* tangent space at a germ $(x(r), z(r))$ generated by the restricted left diffeomorphisms $(g(x, z), h(z)) : \mathbb{R}^2 \rightarrow \mathbb{R}^2$, where $g : \mathbb{R}^2 \rightarrow \mathbb{R}$, $h : \mathbb{R} \rightarrow \mathbb{R}$ are any germs. For instance, the left space T^l at (r^2, r^3) of \prec is formed by $(g(r^2, r^3), h(r^3)) = (a_1 + a_2 r^2 + a_3 r^3 + \dots, b_1 + b_2 r^3 + \dots)$. The *parameter* normal space N^p of a deformation $F(r; a, b)$ consists of linear combinations $c \frac{\partial F}{\partial a} + d \frac{\partial F}{\partial b}$ at $a = b = 0$, where c, d are constants, e.g. the space N^p of $(r^5 + ar^3 + br, r^2)$ consists of vectors $(cr^3 + dr, 0)$.

In the case of a multi-germ the right space T_i^r is associated to the independent right diffeomorphisms $f_i(r)$ around each point r_i . The left space T_i^l is generated by the same left diffeomorphisms at every r_i . The parameter space N_i^p is spanned by the derivatives along the parameters of the deformation at each r_i .

The following standard statement is a simple application of [1, section I.8.2].

Proposition 4.2. *A deformation $F(r; a, b)$ of a multi-germ $(x(r), z(r)) : \mathbb{R} \rightarrow \mathbb{R}^2$ is versal if at every point r_i any germ $\mathbb{R} \rightarrow \mathbb{R}^2$ can be represented as a sum of vectors from the spaces T_i^r , T_i^l and N_i^p .* \square

Lemma 4.3. *The codimension 2 singularities from Definition 3.4 have the versal deformations with parameters a, b in the table below.*

\ast, \mathcal{A}_e	$\{x = 0, z = r\}, \{x = r + a, z = r\}, \{x = -r - b, z = r\}, \{x = er, z = r\}$
\bowtie, \mathcal{A}_e	$\{x = r^2 - 2a, z = r\}, \{x = 0, z = r\}, \{x = r - b, z = r\}$
\succ, \mathcal{A}_e	$\{x = r^3 - br, z = r^2\}, \{x = r - a, z = r\}$
\bowtie, \mathcal{A}_e	$\{x = r^3 - 3br + a, z = r\}, \{x = 0, z = r\}$
\bowtie, \mathcal{A}_e	$\{x = r^5 + ar^3 + br, z = r^2\}$
\prec, \mathcal{A}_z	$\{x = r^2, z = r^3 + ar^2 - br\}$
\bowtie, \mathcal{A}_z	$\{x = r, z = r^2 - b\}, \{x = r + a, z = -r^2\}$
\bowtie, \mathcal{A}_z	$\{x = r, z = -2r^2 - b\}, \{x = r + a, z = -r^2\}$
\bowtie, \mathcal{A}_z	$\{x = r, z = -r^2\}, \{x = r + a, z = r\}, \{x = -r - b, z = r\}$
\bowtie, \mathcal{A}_z	$\{x = r, z = -r^2\}, \{x = r + a, z = r\}, \{x = r/2 - b, z = r\}$

Sketch. Versal deformations of classical codimension 2 singularities $\curvearrowright (A_4)$, $\curvearrowleft (D_5)$, $\times (D_4)$, $\lrcorner (A_5)$ and $\ast (X_9)$ up to \mathcal{A}_e -equivalence were recently described by Wall [14, subsection 6.1]. The remaining cases follow from the table below.

singularity	T_i^r	T_i^l	N_i^p
\curvearrowleft	$(2rf(r), 3r^2f(r))$	$(g(r^2, r^3), h(r^3))$	$(0, cr^2 - dr)$
\times	$(f_1(r), 2rf_1(r))$ $(f_2(r), -2rf_2(r))$	$(g(r, r^2), h(r^2))$ $(g(r, -r^2), h(-r^2))$	$(0, -d)$ $(c, 0)$
\lrcorner	$(f_1(r), -4rf_1(r))$ $(f_2(r), -2rf_2(r))$	$(g(r, -2r^2), h(-2r^2))$ $(g(r, -r^2), h(-r^2))$	$(0, -d)$ $(c, 0)$
\lrcorner	$(f_1(r), -2rf_1(r))$ $(f_2(r), f_2(r))$ $(-f_3(r), f_3(r))$	$(g(r, -r^2), h(-r^2))$ $(g(r, r), h(r))$ $(g(-r, r), h(r))$	$(0, 0)$ $(c, 0)$ $(-d, 0)$
\lrcorner	$(f_1(r), -2rf_1(r))$ $(f_2(r), f_2(r))$ $(-f_3(r)/2, f_3(r))$	$(g(r, -r^2), h(-r^2))$ $(g(r, r), h(r))$ $(g(-r/2, r), h(r))$	$(0, 0)$ $(c, 0)$ $(-d, 0)$

Case vi of a horizontal cusp \curvearrowleft . By Proposition 4.2 we should prove that any germ $(x(r), z(r)) : \mathbb{R} \rightarrow \mathbb{R}^2$ can be represented as a sum of vectors from the spaces T_1^r , T_1^l and N_1^p , i.e. we solve the functional equations from the table $x(r) = 2rf(r) + g(r^2, r^3)$ and $z(r) = -dr + cr^2 + 3r^2f(r) + h(r^3)$, which have one of the possible solutions

$$\begin{cases} d = -\dot{z}(0), & h(r^3) = z(0), & f(r) = \frac{z(r) - \dot{z}(0)r - z(0)}{3r^2} + \frac{\dot{x}(0)}{2} - \frac{\ddot{z}(0)}{6}, \\ c = \frac{\ddot{z}(0) - 3\dot{x}(0)}{2}, & g(r^2, r^3) = x(r) - \dot{x}(0)r - 2\frac{z(r) - \ddot{z}(0)r^2/2 - \dot{z}(0)r - z(0)}{3r} \end{cases}$$

Here h has only the constant term and $g(r^2, r^3)$ has no linear term in r , all other powers have the form $2j + 3k$ for some integers $j, k \geq 0$, e.g.

for a germ $(a_0 + a_1r + a_2r^2 + \dots, b_0 + b_1r + b_2r^2 + \dots)$ one has

$$f = a_1/2 + \dots, \quad g(x, z) = a_0 + a_2x + \dots, \quad h = b_0, \quad d = -b_1, \quad c = (2b_2 - 3a_1)/2.$$

Case vii of a mixed tangency \times . We prove that at each point r_i , $i = 1, 2$, any germ $(x_i, z_i) : \mathbb{R} \rightarrow \mathbb{R}^2$ can be represented as a sum of vectors from T_i^r , T_i^l , N_i^p , i.e. in terms of suitable c, d and f, g, h . Write down the equations from the table above.

$$(\times) \quad \begin{cases} x_1(r) = f_1(r) + g(r, r^2), & z_1(r) = 2rf_1(r) + h(r^2) - d, \\ x_2(r) = c + f_2(r) + g(r, -r^2), & z_2(r) = -2rf_2(r) + h(-r^2). \end{cases}$$

For a function $f(r)$ denote its constant term simply by f . The equations $z_1(r) = 2rf_1(r) + h(r^2) - d$ and $z_2(r) = -2rf_2(r) + h(-r^2)$ in degree 1 determine the constant terms f_1, f_2 of $f_1(r), f_2(r)$. Then system (\times) in degree 0 has a unique solution:

$$(\times)_0 \quad \begin{cases} x_1 = f_1 + g, & z_1 = h - d, & \begin{cases} g = x_1 - f_1, & h = z_2, \\ c = x_2 - x_1 + f_1 - f_2, & d = z_2 - z_1. \end{cases} \end{cases}$$

For a function $f(r)$ define its odd and even part as $\text{Odd } f(r) = \frac{f(r) - f(-r)}{2}$,

Even $f(r) = \frac{f(r) + f(-r)}{2}$. We look for solutions $g(x, z) = g_1(x) + g_2(z)$ and $h(z)$

such that $g_2(-z) = -g_2(z)$, $h(z) = h(-z)$. Split each equation of (\succ) :

$$\begin{cases} \text{Odd } x_1(r) = \text{Odd } f_1(r) + \text{Odd } g_1(r), & \text{Even } z_1(r) = 2r\text{Odd } f_1(r) + h(r^2) - d, \\ \text{Even } x_1(r) = \text{Even } f_1(r) + \text{Even } g_1(r) + g_2(r^2), & \text{Odd } z_1(r) = 2r\text{Even } f_1(r), \\ \text{Odd } x_2(r) = \text{Odd } f_2(r) + \text{Odd } g_1(r), & \text{Even } z_2(r) = -2r\text{Odd } f_2(r) + h(r^2) \\ \text{Even } x_2(r) = c + \text{Even } f_2(r) + \text{Even } g_1(r) - g_2(r^2), & \text{Odd } z_2(r) = -2r\text{Even } f_2(r). \end{cases}$$

The resulting system has a solution below, where $\text{Even } z_1(r) - \text{Even } z_2(r) + d$ is divisible by r due to (\succ_0) . So the deformation is versal by Proposition 4.2.

$$\begin{cases} \text{Even } f_1(r) = \text{Odd } z_1(r)/2r, & \text{Even } f_2(r) = -\text{Odd } z_2(r)/2r, \\ \text{Odd } f_1(r) = (\text{Even } z_1(r) - \text{Even } z_2(r) + d)/4r + (\text{Odd } x_1(r) - \text{Odd } x_2(r))/2, \\ \text{Odd } f_2(r) = (\text{Even } z_1(r) - \text{Even } z_2(r) + d)/4r + (\text{Odd } x_2(r) - \text{Odd } x_1(r))/2, \\ \text{Even } g_1(r) = (\text{Even } x_1(r) + \text{Even } x_2(r) - \text{Odd } z_1(r)/2r + \text{Odd } z_2(r)/2r - c)/2, \\ \text{Odd } g_1(r) = (+\text{Even } z_2(r) - \text{Even } z_1(r) - d)/4r + (\text{Odd } x_1(r) + \text{Odd } x_2(r))/2, \\ g_2(r^2) = (\text{Even } x_1(r) - \text{Even } x_2(r) - \text{Odd } z_1(r)/2r - \text{Odd } z_2(r)/2r + c)/2, \\ h(r^2) = (\text{Even } z_1(r) + \text{Even } z_2(r) + d)/2 + r(\text{Odd } x_2(r) - \text{Odd } x_1(r)). \end{cases}$$

Case viii of an extreme tangency \blacklozenge is similar to Case vii.

Case ix of a horizontal triple point \blacklozenge . The table above gives

$$(\blacklozenge) \quad \begin{cases} x_1(r) = f_1(r) + g(r, -r^2), & z_1(r) = -2rf_1(r) + h(-r^2), \\ x_2(r) = c + f_2(r) + g(r, r), & z_2(r) = f_2(r) + h(r), \\ x_3(r) = -d - f_3(r) + g(-r, r), & z_3(r) = f_3(r) + h(r). \end{cases}$$

The equation $z_1(r) = -2rf_1(r) + h(-r^2)$ in degree 1 determines the constant term f_1 of the function $f_1(r)$. Then system (\blacklozenge) in degree 0 has a unique solution.

$$\begin{cases} x_1 = f_1 + g, & z_1 = h, \\ x_2 = c + f_2 + g, & z_2 = f_2 + h, \\ x_3 = -d - f_3 + g, & z_3 = f_3 + h. \end{cases} \quad \begin{cases} g = x_1 - f_1, & h = z_1, \\ f_2 = z_2 - z_1, & c = x_2 - x_1 + f_1 + z_1 - z_2, \\ f_3 = z_3 - z_1, & d = x_1 - f_1 - x_3 + z_1 - z_3. \end{cases}$$

We look for $g(x, z) = g_1(x) + g_2(z)$. Apply elementary operations to (\blacklozenge)

$$(\blacklozenge_1) \quad \begin{cases} 2rx_1(r) + z_1(r) = 2rg_1(r) + 2rg_2(-r^2) + h(-r^2), \\ x_2(r) - z_2(r) = c + g_1(r) + g_2(r) - h(r), \\ x_3(r) + z_3(r) = -d + g_1(-r) + g_2(r) + h(r). \end{cases}$$

The functions f_1, f_2, f_3 can be expressed in terms of the solutions of (\blacklozenge_1) . Split the 1st equation of (\blacklozenge_1) into the odd and even parts, then apply operations to (\blacklozenge_1) :

$$2r\text{Odd } x_1(r) + \text{Even } z_1(r) = 2r\text{Odd } g_1(r) + h(-r^2),$$

$$(\blacklozenge_2) \quad 2r\text{Even } x_1(r) + \text{Odd } z_1(r) = 2r\text{Even } g_1(r) + 2rg_2(-r^2),$$

$$x_3(r) + z_3(r) + x_2(r) - z_2(r) - 2\text{Even } x_1(r) - \frac{\text{Odd } z_1(r)}{r} = c - d + 2g_2(r) - 2g_2(-r^2),$$

which determines the coefficients of $g_2(r) = \sum_{i=0}^{\infty} e_i r^i$ splitting into parts as follows. Taking the odd part, we compute e_i with all odd i , then consider terms with powers $4i$ and $4i + 2$ separately, find all e_{4i+2} and continue splitting into parts. Having found $g_2(r)$, compute $\text{Even } g_1(r)$ from (\blacklozenge_2) and work out $h(r)$, $\text{Odd } g_1(r)$ from

$$\begin{cases} x_2(r) - z_2(r) - x_3(r) - z_3(r) = c + d + 2\text{Odd } g_1(r) - 2h(r), \\ 2r\text{Odd } x_1(r) + \text{Even } z_1(r) = 2r\text{Odd } g_1(r) + h(-r^2), \end{cases}$$

excluding $\text{Odd } g_1(r)$ and then splitting the result into parts as above.

Case x of another horizontal triple point K is similar to Case ix. \square

4.2. Bifurcation diagrams of codimension 2 singularities.

The *bifurcation* diagram of a codimension 2 singularity δ from Definition 3.4 is formed by the pairs $(a, b) \in \mathbb{R}^2$ from the versal deformation of δ from Lemma 4.3. We will describe curves representing codimension 1 subspaces Σ_γ adjoined to Σ_δ in the space SL of all links $K \subset V$.

Oriented arcs in bifurcation diagrams of Figure 8 are associated to canonical loops $\text{CL}(K_{\pm\epsilon}) \subset \text{SL}$, where links $K_{\pm\epsilon}$ are close to a given link K_0 . At the zero critical moment, the loop $\text{CL}(K_0)$ defines an arc through the origin $\{a = b = 0\}$. These arcs are transversal to the codimension 1 subspace $\Sigma^{(1)}$ apart from the cases below. In Figure 8ix and 8x the canonical loop $\text{CL}(K_s)$ is *parallel* to Σ_{V} , Σ_{X} , Σ_{J} in the following sense: if $K \in \Sigma_{\text{V}}$, then $\text{CL}(K) \subset \Sigma_{\text{V}} \cup \Sigma_{\text{X}}$. If $K \in \Sigma_{\text{X}}$, then $\text{CL}(K) \subset \Sigma_{\text{X}} \cup \Sigma_{\text{J}}$. Similarly, $K \in \Sigma_{\text{J}}$ implies that $\text{CL}(K) \subset \Sigma_{\text{J}} \cup \Sigma_{\text{K}}$.

Lemma 4.4. *Figure 8 contains the bifurcation diagrams of the codimension 2 singularities $\delta : \text{K}, \text{X}, \text{V}, \text{J}, \text{N}, \text{K}, \text{X}, \text{J}, \text{N}, \text{K}$ and shows how the canonical loops $\text{CL}(K_{\pm\epsilon})$ intersect the adjoined codimension 1 subspaces Σ_γ .*

Proof. In Cases i–v below the canonical loops transversally intersects all the singular subspaces since the tangents of intersecting arcs are not horizontal.

Case i of a quadruple point K . There are 4 singular subspaces Σ_{K} intersecting each other transversally at the singular subspace Σ_{K} . Using the normal form of K from Lemma 4.1, we show 4 subspaces in the bifurcation diagram of Figure 8i, namely $\{a = 0\}$ (branches 1, 2, 4 intersect), $\{b = 0\}$ (branches 1, 3, 4 intersect), $\{a = b\}$ (branches 1, 2, 3 intersect), $\{e(a + b) = b - a\}$ (branches 2, 3, 4 intersect).

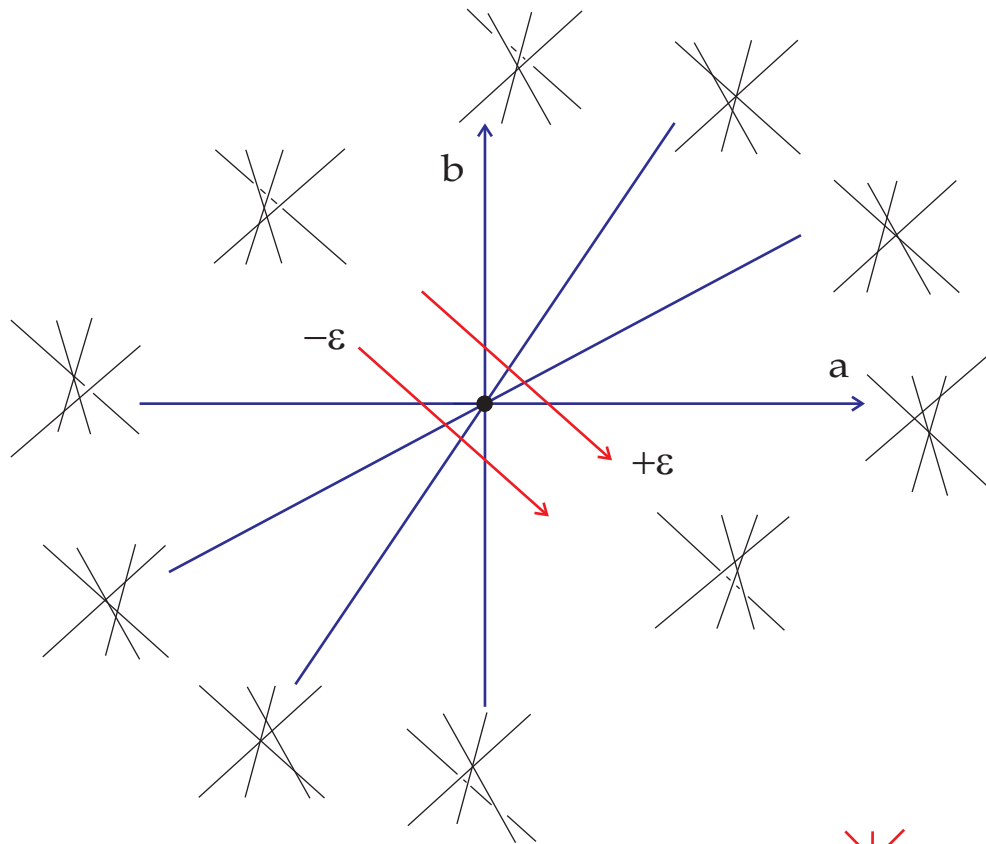
Case ii of a tangent triple point X . The branches $\{x = z^2 - a\}$, $\{x = 0\}$ have a tangency if $a = 0$. The triple point appears when $z^2 - a = 0 = z - b$, i.e. $a = b^2$. The bifurcation diagram of Figure 8ii has 1 parabola and 1 line touching each other.


Case iii of an intersected cusp V . The branch $(r^3 - br, r^2)$ has a self-intersection at $r = \pm\sqrt{b}$, $b \geq 0$, which becomes an ordinary cusp if $b = 0$. The self-intersection is a triple point when it is on the branch $(r - a, r)$, i.e. $a = b$. Finally, we get a simple tangency of $(r^3 - br, r^2)$ and $(r - a, r)$ if $a = 2r^3 - r^2$, $b = 3r^2 - 2r$ or $3a - 2br = r^2$ has a double root, i.e. $b^2 + 3a = 0$. The bifurcation diagram of Figure 8iii contains 1 parabola, 1 line and 1 ray meeting at 0.

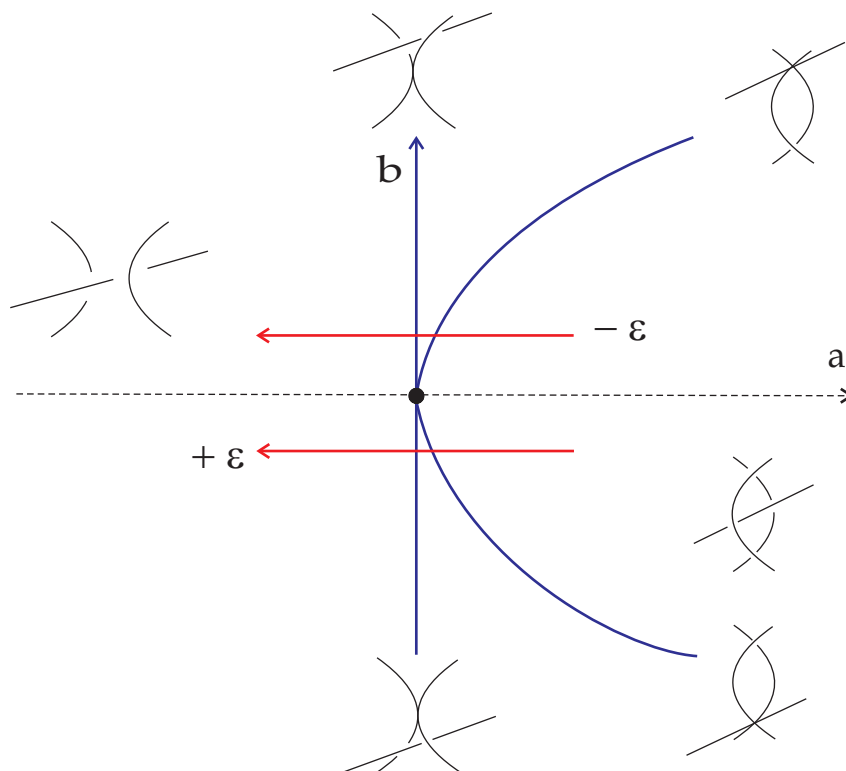
Case iv of a cubic tangency J . The branch $(r^3 - 3br + a, r)$ has extrema of the x -coordinate at $r = \pm\sqrt{b}$, which lie on $(0, r)$ if $r^3 - 3br + a = 0$, i.e. $a^2 = 4b^3$. The only subspace Σ_{X} is adjoined to Σ_{J} in the bifurcation diagram of Figure 8iv.


Case v of a ramphoidal cusp N . The curve $(r^5 + ar^3 + br, r^2)$ has an ordinary cusp when $\dot{x} = \dot{z} = 0$, i.e. $r = 0$ and $b = 0$, and a self-tangency when $5r^4 + 3ar^2 + b = 0$ has two double roots, i.e. $9a^2 = 20b$. The bifurcation diagram of Figure 8v contains 1 parabola and 1 line touching each other at 0.

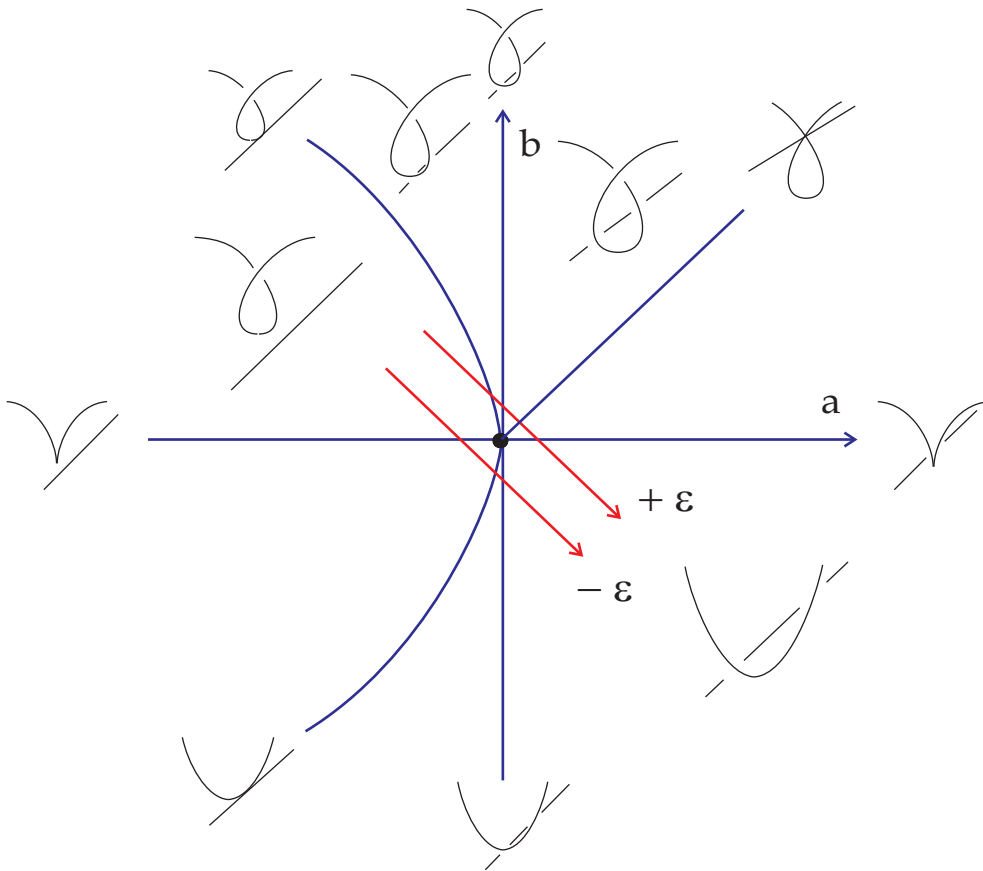
Case vi of a horizontal cusp K . The curve $(r^2, r^3 + ar^2 - br)$ has a crossing at $\pm r$, hence $r^3 = br$ and $r = \pm\sqrt{b}$, $b > 0$. This crossing is critical, i.e. $\dot{z} = 3r^2 + 2ar - b = 0$, if $b = a^2$. The critical point becomes degenerate, i.e. $\ddot{z} = 6r + 2a = 0$, if $b = -a^2/3$.



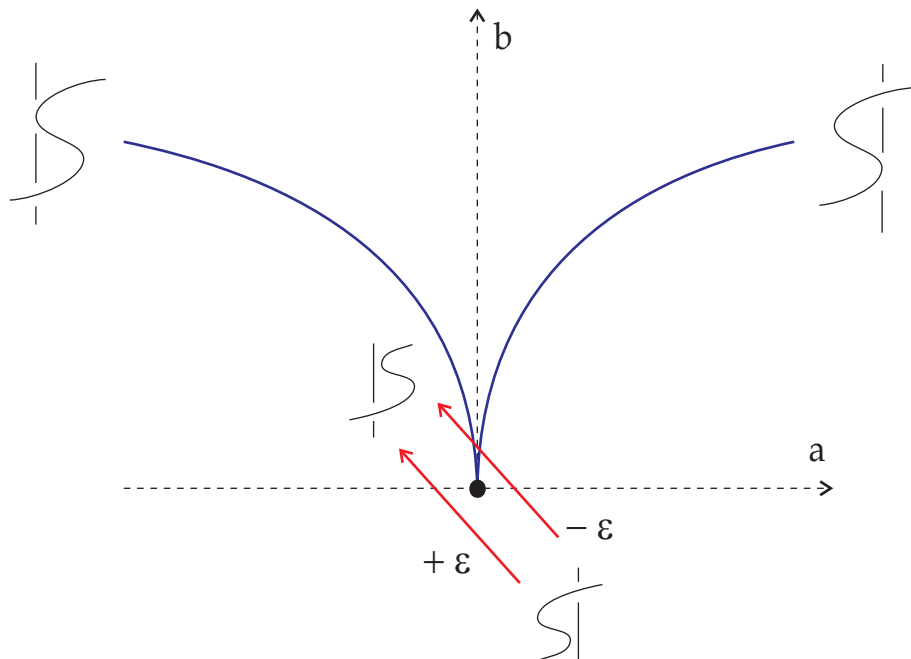
8i: the bifurcation diagram of a quadruple point 



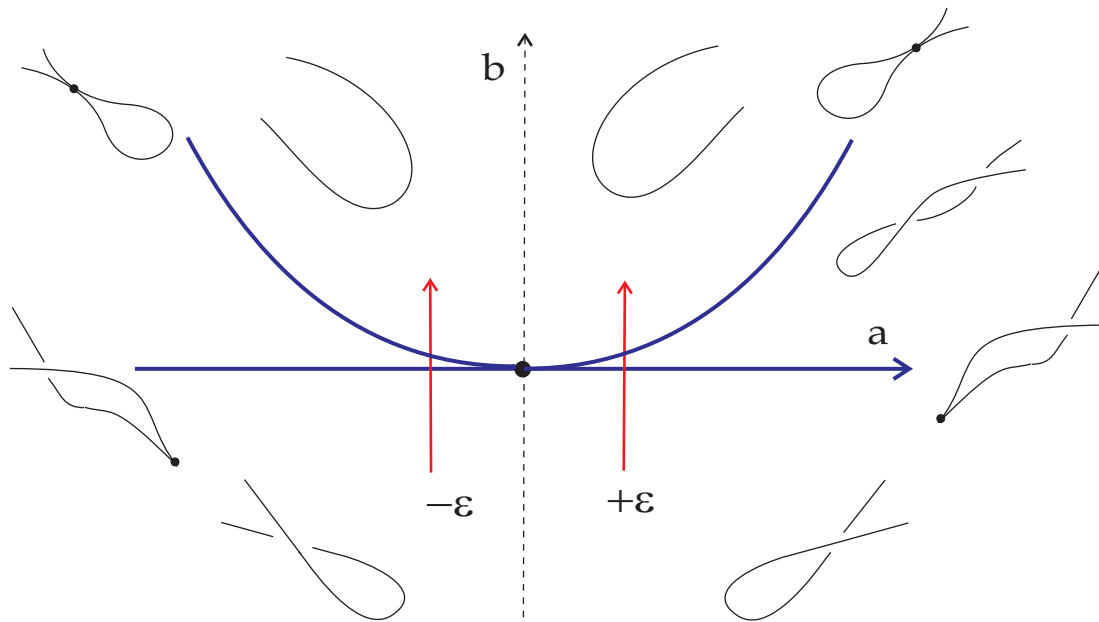
8ii: the bifurcation diagram of a tangent triple point 



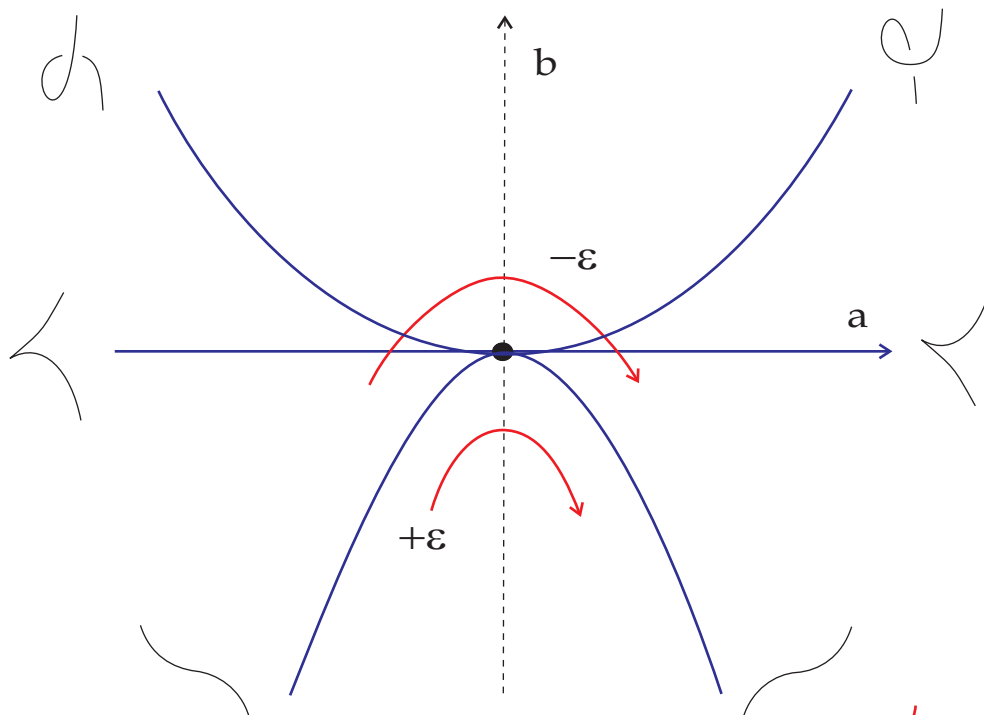
8iii: the bifurcation diagram of an intersected cusp



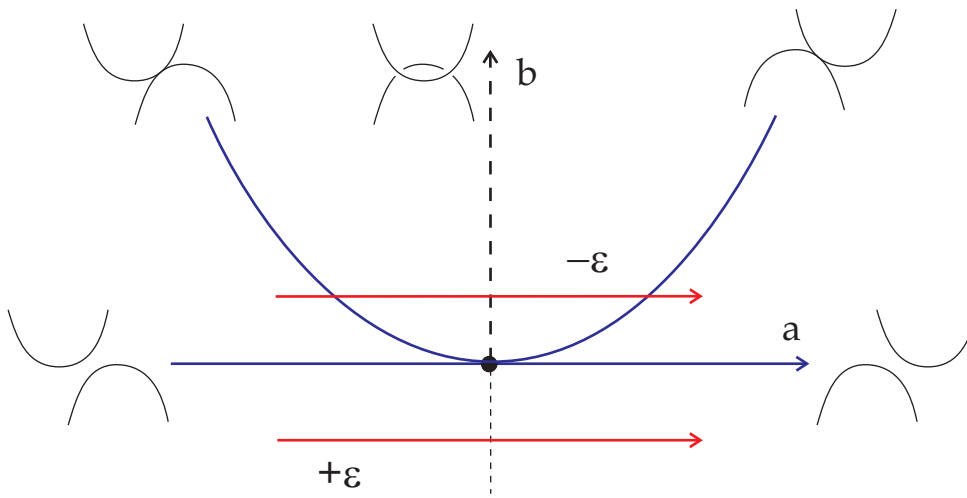
8iv: the bifurcation diagram of a cubic tangency




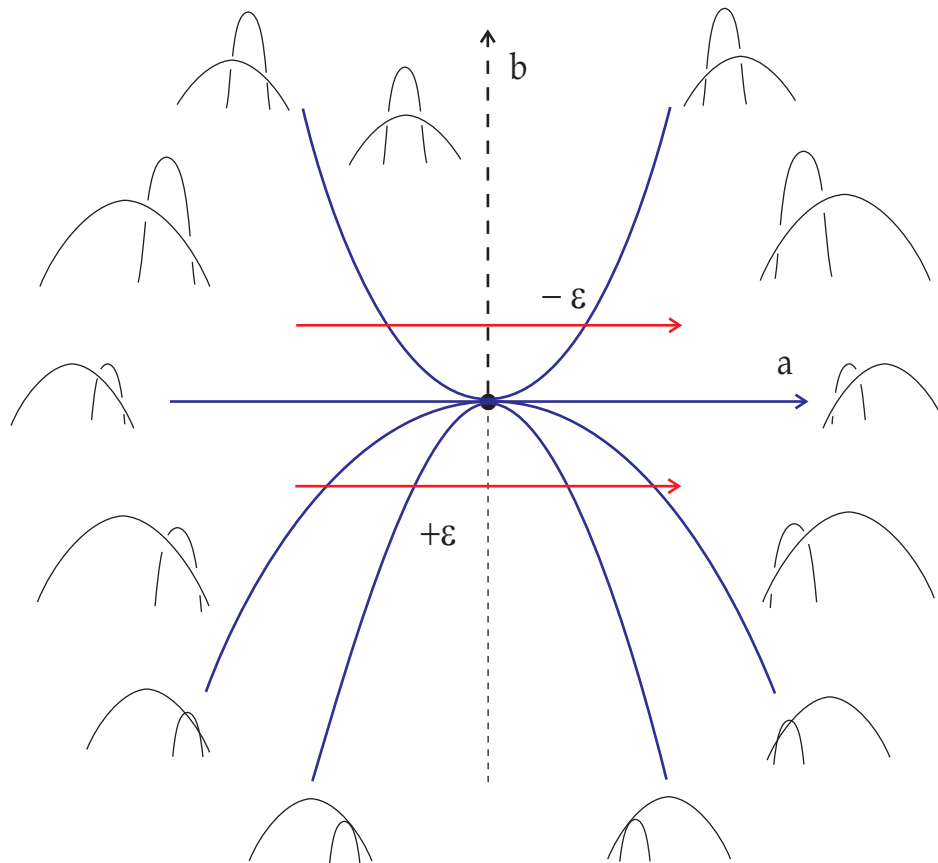
8v: the bifurcation diagram of a ramphoidal cusp



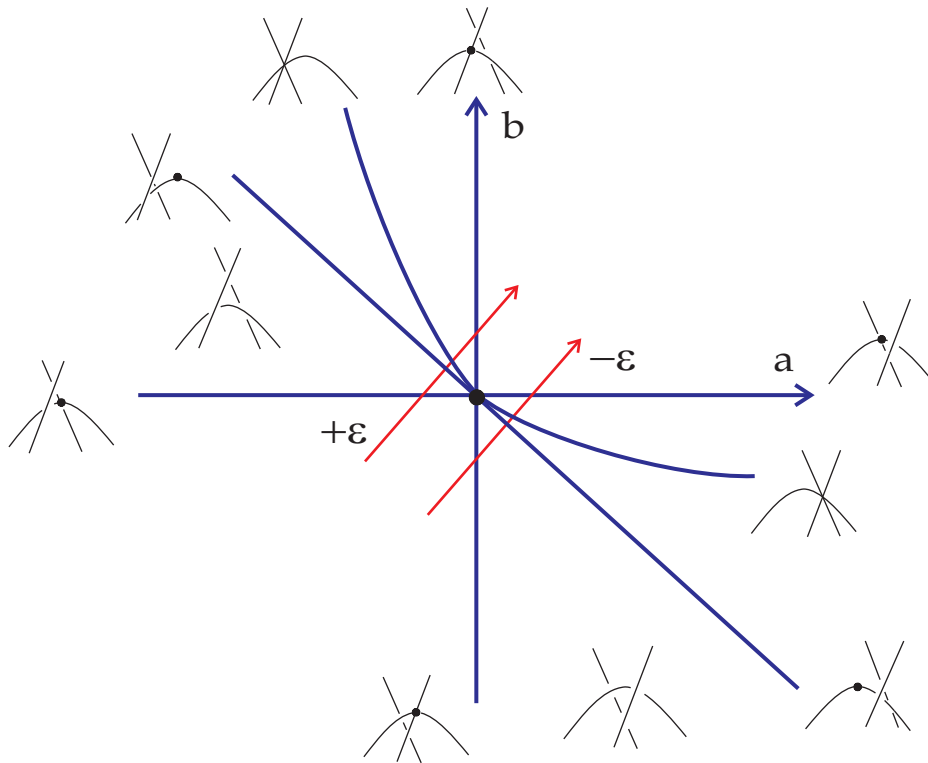
8vi: the bifurcation diagram of a horizontal cusp




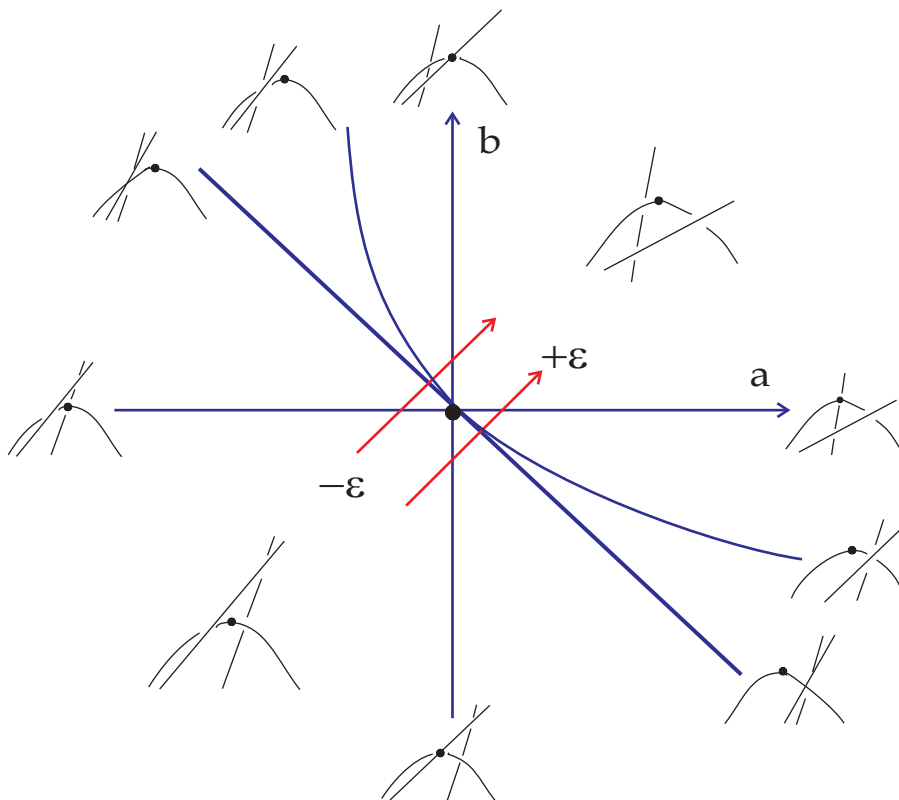
8vii : the bifurcation diagram of a mixed tangency 



8viii : the bifurcation diagram of an extreme tangency 



8ix: the bifurcation diagram of a horizontal triple point 




8x: the bifurcation diagram of a horizontal triple point 

FIGURE 8. Bifurcation diagrams of codimension 2 singularities

The subspace $\Sigma_{\curvearrowright}$ of ordinary cusps, where $\dot{x} = \dot{z} = 0$, is represented by $\{b = 0\}$. The bifurcation diagram of Figure 8vi shows 2 parabolas, 1 line and 1 ray meeting at 0. The arc associated to a canonical loop moves in the vertical direction and remains parallel to the parabola $\{b = -a^2/3\}$ representing the subspace $\Sigma_{\curvearrowright}$.

Case vii of a mixed tangency \curvearrowright . The branch $(r, r^2 - b)$ touches $(r + a, -r^2)$ if $r^2 - b = -(r + a)^2$ has a double root, i.e. $a^2 = 2b$. Both curves have extrema in the same horizontal line when $b = 0$. The bifurcation diagram of Figure 8vii has 1 parabola and 1 line touching each other at 0.

Case viii of an extreme tangency \frown . The branch $(r, -2r^2 + b)$ touches $(r + a, -r^2)$ if $-2r^2 + b = -(r + a)^2$ has a double root, i.e. $2a^2 + b = 0$. Both branches have extrema in the same horizontal line when $b = 0$. The branch $(r, -2r^2 + b)$ passes through an extremum of $(r + a, -r^2)$ at $r = 0$ if $b = 2a^2$. The branch $(r + a, -r^2)$ passes through an extremum of $(r, -2r^2 + b)$ at $r = 0$ if $b = -a^2$. The bifurcation diagram of Figure 8viii has 3 parabolas and 1 line touching each other at 0.

Case ix of a horizontal triple point \bowtie . The branches $(r + a, r)$ and $(-r - b, r)$ pass through the extremum of $(r, -r^2)$ at $r = 0$ when $a = 0$ and $b = 0$, respectively. The crossing of $(r + a, r)$ and $(-r - b, r)$ at $r = -(a + b)/2$ lies in the same horizontal line with the extremum of $(r, -r^2)$ at $r = 0$ if $a + b = 0$. The branches $(r, -r^2)$, $(r + a, r)$ and $(-r - b, r)$ have a triple point if $r = -r^2 + a = r^2 - b$ or $(a - b)^2 = 2(a + b)$, which is a parabola in the bifurcation diagram of Figure 8ix. The arc associated to a canonical loop is transversal to the subspaces, because only one tangent remains horizontal under the rotation.

Case x of another horizontal triple point \bowtie is similar to Case ix. □

5. THE DIAGRAM SURFACE OF A LINK

In this section the classification problem of generic links $K \subset V$ reduces to their diagram surfaces $\text{DS}(K)$ in the thickened torus $\mathbb{T} = A_{xz} \times S_t^1$, $A_{xz} = [-1, 1]_x \times S_z^1$.

5.1. The diagram surface of a link and generic surfaces.

Briefly the diagram surface of a loop $\{K_t\}$ of links is the 1-parameter family of the diagrams $\text{pr}_{xz}(K_t) \subset A_{xz} \times \{t\}$. This family can be considered as the union of link diagrams, i.e. as a 2-dimensional surface in the thickened torus $\mathbb{T} = A_{xz} \times S_t^1$.

Definition 5.1. Let $\{K_t\} \subset \text{SL}$ be a loop of links. The *diagram surface* $\text{DS}(\{K_t\}) \subset A_{xz} \times S_t^1$ is formed by the diagrams $\text{pr}_{xz}(K_t) \subset A_{xz} \times \{t\}$, $t \in S_t^1$. If K_t are knots, $\text{DS}(\{K_t\})$ is the torus $S^1 \times S_t^1$ mapped to the thickened torus $\mathbb{T} = A_{xz} \times S_t^1$. The *diagram surface* $\text{DS}(K)$ of an oriented link $K \subset V$ consists of the diagrams $\text{pr}_{xz}(\text{rot}_t(K)) \subset A_{xz} \times \{t\}$ and is oriented by the orientations of K and S_t^1 . ■

Figure 9 shows vertical sections of $\text{DS}(K)$ for a smoothed trefoil K from Figure 2, $t \in [0, \pi]$. Each section is the diagram of a rotated trefoil $\text{rot}_t(K)$ for some $t \in S_t^1$. Local extrema of $\text{rot}_t(K)$ form horizontal circles parallel to S_t^1 . Several arcs in Figure 9 are dashed or dotted, because they are invisible in the x -direction.

By Definition 3.9 the shift $t \mapsto t + \pi$ maps the surface $\text{DS}(\{K_t\})$ to its image under the symmetry in S_z^1 . Actually the link $K_{t+\pi}$ is obtained from K_t by the symmetry rot_π , ie the diagrams $\text{pr}_{xz}(K_{t+\pi})$ and $\text{pr}_{xz}(K_t)$ are symmetric for all $t \in S_t^1$. For a generic loop $\{K_t\}$, the vertical sections of $\text{DS}(K)$ are the diagrams $\text{pr}_{xz}(K_t)$ and

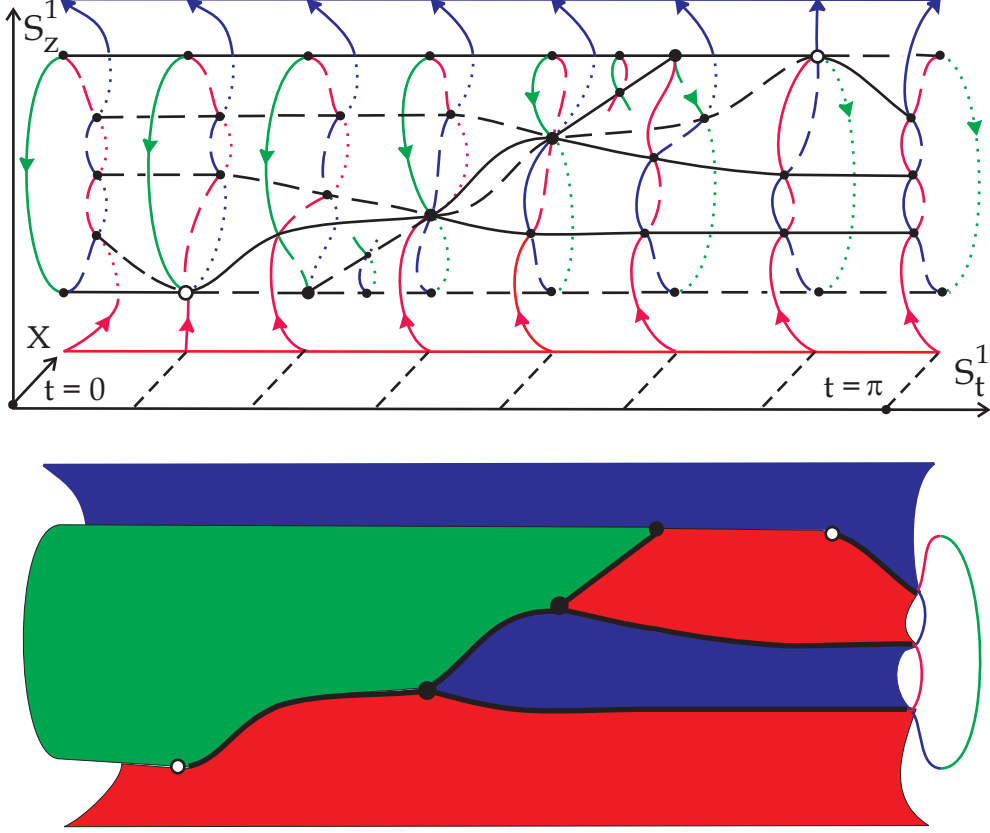


FIGURE 9. Half the diagram surface of a smoothed trefoil from Figure 2.

allow the codimension 1 singularities $\bowtie, \bowtie, \gamma, \blacklozenge$ only. It follows from the fact that any critical point of $\text{pr}_z : K_t \rightarrow S_z^1$ remains critical under rot_t .

For any $t \in S_t^1$, the points from $K_t \cap (D_{xy} \times \{z = \pm 1\})$ and the critical points of $\text{pr}_z : K_t \rightarrow S_z^1$ divide the i -th component of K_t into arcs $A_{t,i,q}$, $q = 1, \dots, n_i$. The total number of these arcs does not depend on t since any critical point $a_t \in K_t$ of pr_z remains critical while t varies. The union $\cup a_t$ of the extrema of $\text{pr}_z : K_t \rightarrow S_z^1$ for all $t \in S_t^1$ splits into *critical circles* C_i of $\text{DS}(\{K_t\})$. The union $B_{i,q} = \cup A_{t,i,q}$ over all $t \in S_t^1$ is called a *trace band* of $\text{DS}(\{K_t\})$. The 3 trace bands in the bottom picture of Figure 9 have different colours. The arcs $A_{t,i,q}$ are monotonic with respect to $\text{pr}_{zt} : K_t \rightarrow S_z^1 \times \{t\}$. Then the trace bands project 1-1 under $\text{pr}_{zt} : \text{DS}(\{K_t\}) \rightarrow S_z^1 \times S_t^1$. Successive bands $B_{i,q}, B_{i+1,q}$ meet at a critical circle.

The *singular* points of $\text{DS}(\{K_t\})$ are crossings and codimension 1 singularities of the diagrams $\text{pr}_{xz}(K_t)$ over all $t \in S_t^1$. A *trace arc* is an intersection of the interiors of 2 trace bands in $\text{DS}(\{K_t\})$. The triple points, tangent points, cusps and critical crossings of link diagrams $\text{pr}_{xz}(K_t)$ are called *triple* vertices, *tangent* vertices, *hanging* vertices and *critical* vertices of $\text{DS}(\{K_t\})$, respectively. So a trace arc may contain several vertices of $\text{DS}(\{K_t\})$ in the usual sense.

Take a singular point $p \in \text{DS}(K)$ that is not a vertex and does not belong to a critical circle of $\text{DS}(K)$. Then p is a double crossing of two arcs $A_{t,i,q}$ and $A_{t,j,s}$ in a diagram $\text{pr}_{xz}(K_t)$. If the arc $A_{t,i,q}$ passes over (respectively, under) $A_{t,j,s}$ then associate to p the label $(q_i s_j)$ (respectively, the *reversed* label $(s_j q_i)$). If K_t is a knot then we miss the indices $i, j = 1$ as in Figure 3.

Trace arcs of $DS(\{K_t\})$ end at hanging vertices, meet each other at critical vertices and intersect at triple vertices. Each trace arc of $DS(K)$ is the evolution trace of a double crossing in $A_{xz} \times S_t^1$ while t varies. The label of a point p does not change when p passes through tangent vertices and triple vertices.

The diagram surface can be defined for any loop of links and can be extremely complicated. The surfaces corresponding to generic loops are simple and play the role of general link diagrams in dimension 3. As in the case of links, we define a generic surface associated to a generic loop. A generic surface will be an immersed surface with all combinatorial features of diagram surfaces of generic loops. For any generic surface, a corresponding generic loop is constructed in Lemma 5.6.

Definition 5.2. Decompose S_i^1 into arcs $A_{i,1}, \dots, A_{i,n_i}$. Introduce the *trace bands* $B_{i,q} = A_{i,q} \times S_t^1$, $q = 1, \dots, n_i$. A *generic surface* S is the image of a smooth map $h : (\sqcup_{i=1}^m S_i^1) \times S_t^1 = \cup_{i=1}^m (\cup_{q=1}^{n_i} B_{i,q}) \rightarrow A_{xz} \times S_t^1$ such that Conditions (i)–(v) hold

(i) **Conditions** on *symmetry* and *trace bands*.

- under $t \mapsto t + \pi$ the surface S maps to its image under the symmetry in S_z^1 ;
- each trace band $B_{i,q} \subset S$ projects one-to-one under $\text{pr}_{zt} : S \rightarrow S_z^1 \times S_t^1$.

The surface S should be simple enough. More formally we require the following.

(ii) **Conditions** on *sections* $D_t = S \cap (A_{xz} \times \{t\})$, $t \in S_t^1$.

There are finitely many critical moments $t_1, \dots, t_l \in S_t^1$ such that

- for all $t \notin \{t_1, \dots, t_l\}$, the sections $\{D_t\}$ are general diagrams;
- for each $t = t_1, \dots, t_l$, the section D_t has one of the singularities $\bowtie, \bowtie, \gamma, \hookleftarrow$;
- while t passes a critical moment, D_t changes by a move I–IV in Figure 5.

Conditions (ii) on sections imply some restrictions on trace bands. These requirements can be stated independently to define trace arcs and critical circles.

(iii) **Conditions** on *trace arcs* and *critical circles*:

- a *trace arc* is an intersection of the interiors of 2 trace bands $B_{i,q}$ and $B_{j,s}$;
- a *critical circle* $C_{i,q}$ is the common boundary of successive bands $B_{i,q}, B_{i,q+1}$;

The arcs defined above allow us to introduce vertices of a generic surface S .

(iv) **Conditions** on *vertices*:

- a *triple vertex* is a transversal intersection of 3 trace bands $B_{i,q}, B_{j,s}, B_{k,r}$;
- a *hanging vertex* of S is the endpoint of a trace arc in $B_{i,q} \cap B_{i,q+1}$;
- a *critical vertex* is the intersection of a critical circle $C_{i,q}$ and $B_{j,s} \not\supset C_{i,q}$;
- a *tangent vertex* is a critical point of pr_t on the interior of a trace arc;
- all the *vertices* are distinct and map on different points under $\text{pr}_t : S \rightarrow S_t^1$.

Finally fix labels (i, q) and (j, s) . Take a trace arc from the intersection $B_{i,q} \cap B_{j,s}$ of interiors of 2 trace bands. Endow the chosen arc with a *label*: either $(q_i s_j)$ or $(s_j q_i)$ in such a way that the following restrictions apply.

(v) **Conditions** on *labels*:

- under the time shift $t \mapsto t + \pi$, each label reverses: $(q_i s_j) \mapsto (s_j q_i)$;

- trace arcs intersecting at a triple vertex are endowed with $(q_i s_j), (s_j r_k), (q_i r_k)$;
- a hanging vertex is endowed with the label of the trace arc containing it;
- each circle $C_{i,q}$ has 2 hanging vertices endowed with $((q+1)_i, q_i), (q_i, (q+1)_i)$;
- if a trace band $B_{j,s}$ intersects a critical circle $C_{i,q}$ in a vertex c then the label at c transforms as follows: $(q_i s_j) \leftrightarrow ((q+1)_i, s_j)$ or $(s_j q_i) \leftrightarrow (s_j, (q+1)_i)$. ■

To get the following result compare Definitions 3.9, 5.1 with Definition 5.2.

Lemma 5.3. *For any generic loop L of links, the diagram surface $DS(L)$ is a generic surface in the sense of Definition 5.2.* □

5.2. Three-dimensional moves on generic surfaces.

Definition 5.4. A smooth family of surfaces $\{S_r \subset A_{xz} \times S_t^1\}$, $r \in [0, 1]$, is an *equivalence* if there are finitely many critical moments $r_1, \dots, r_k \in [0, 1]$ such that

- for all non-critical moments $r \notin \{r_1, \dots, r_k\}$, the surfaces S_r are generic;
- if r passes through a critical moment, S_r changes by a move in Figure 10. ■

Each move in Figure 10 denotes 2 symmetric moves since the surfaces S_r are symmetric in S_z^1 under $t \mapsto t + \pi$. The following claim will be proved using bifurcation diagrams of codimension 2 singularities of link diagrams, see Lemma 4.4.

Lemma 5.5. (a) *Suppose that a family of loops $\{L_s\}$, $s \in [-1, 1]$, in the space SL of all links $K \subset V$ transversally intersects the subspace $\Sigma^{(2)}$ at $s = 0$. Then the diagram surface $DS(L_s)$ changes near 0 by a move in Figure 10i–x.*

(b) *If a family of loops $\{L_s\}$, $s \in [-1, 1]$, in the space SL has a simple tangency with Σ_{\bowtie} at $s = 0$, then $DS(L_s)$ changes near 0 by the move in Figure 10xi.*

Sketch. The pictures in Figure 10 are obtained from the corresponding pictures in Figure 8. For instance, in Figure 8iii the canonical loop $CL(K_{-\varepsilon})$ meets 3 subspaces $\Sigma_{\Upsilon}, \Sigma_{\chi}, \Sigma_{\bowtie}$. Therefore the surface $DS(K_{-\varepsilon})$ has three distinguished points: a hanging vertex, a tangent vertex and a critical one as in Figure 10iii. Right after the move when all three points pass through each other, the surface $DS(K_{+\varepsilon})$ has 4 interesting points: three have the previous types, the new one is a triple vertex. This situation agrees with 4 intersections of $CL(K_{+\varepsilon})$ with codimension 1 subspaces in Figure 8iii. The remaining cases are absolutely analogous. □

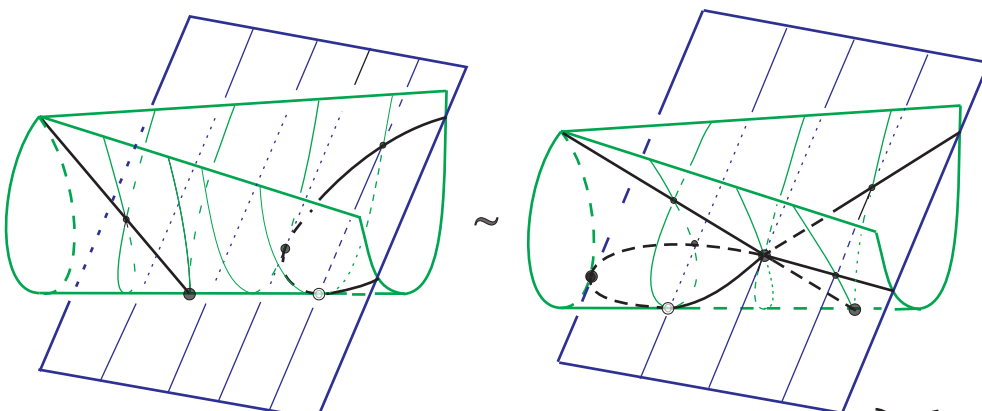
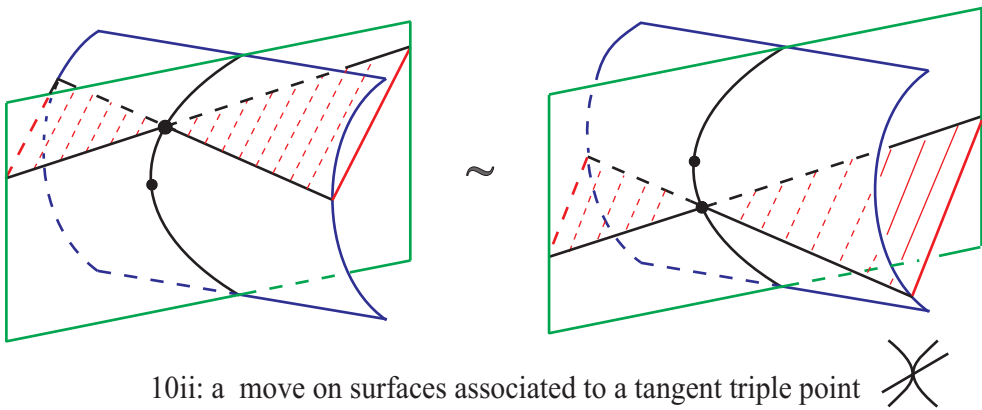
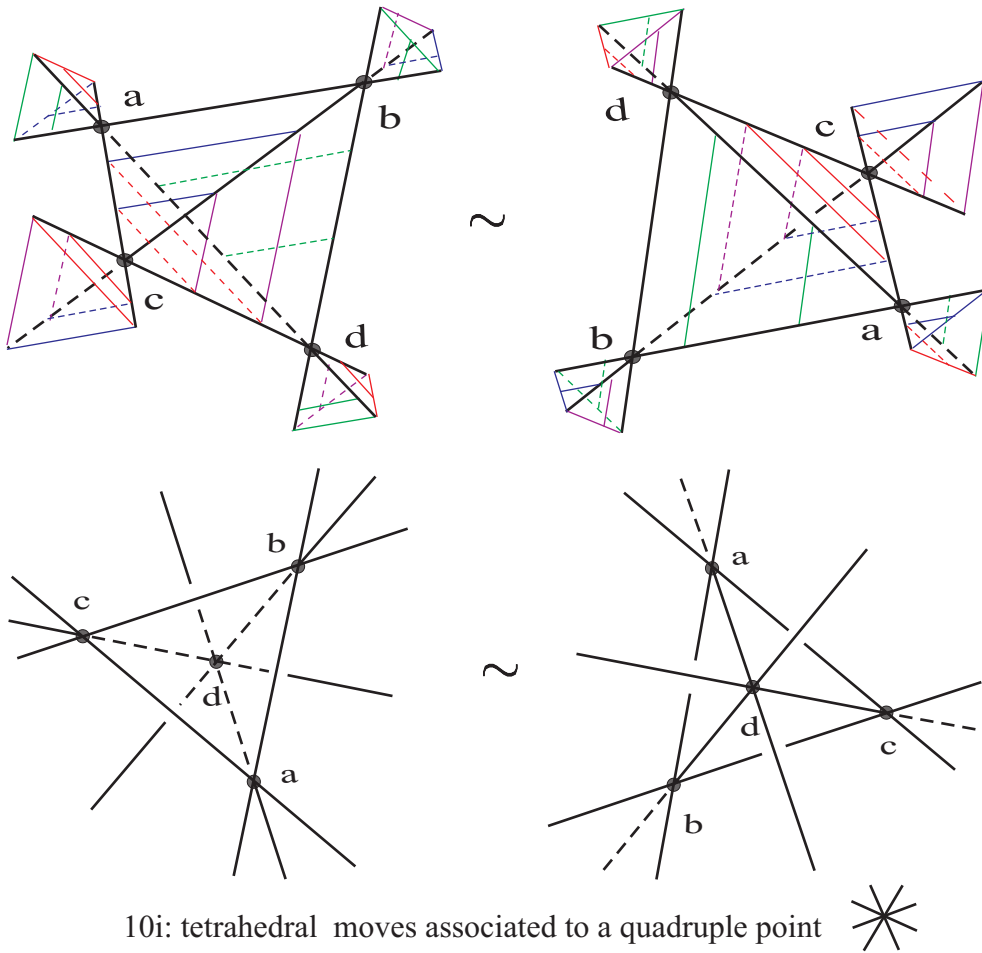
We produced Figure 10 first using our geometric intuition and then justified the moves applying the singularity theory in section 4. Since the family of sections in a generic surface is a general equivalence of diagrams then Lemma 5.6 follows.

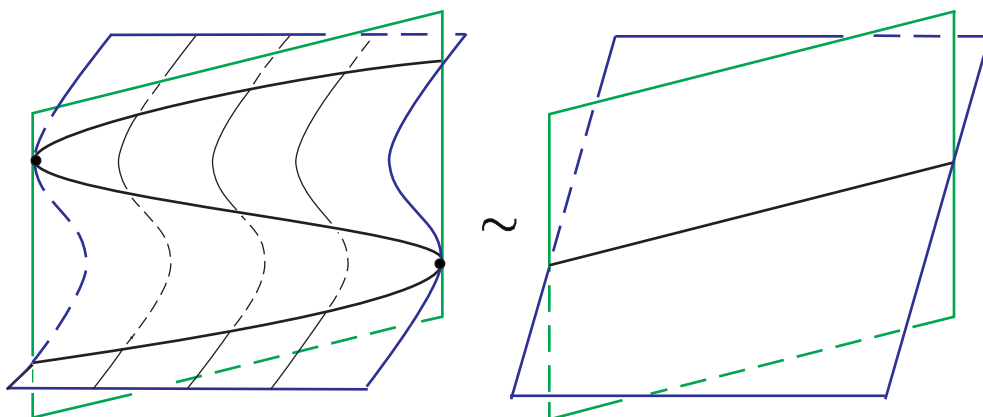
Lemma 5.6. (a) *For any generic surface S , there is a generic loop L of links such that the diagram surface $DS(L)$ coincides with S .*

(b) *For any equivalence of surfaces $\{S_r \subset A_{xz} \times S_t^1\}$, there is a generic homotopy of loops $\{L_r\}$ such that $DS(L_r) = S_r$, $r \in [0, 1]$.* □

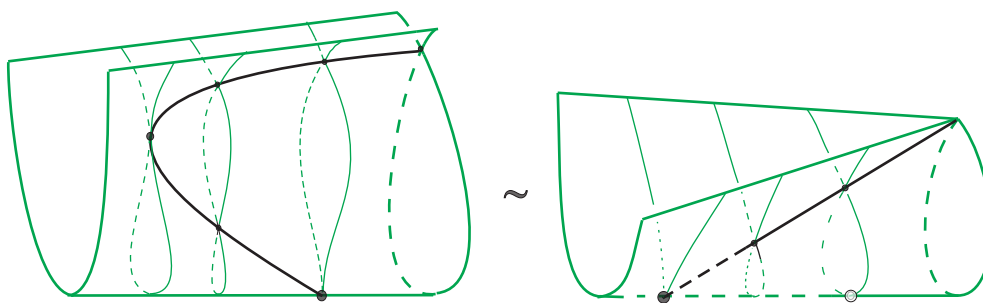
Lemma 5.5 and Definition 3.10 of a generic homotopy imply Lemma 5.7.

Lemma 5.7. *Any generic homotopy of loops $\{L_s\}$, $s \in [0, 1]$ in the space SL provides an equivalence $\{DS(L_s)\}$ of diagram surfaces.* □

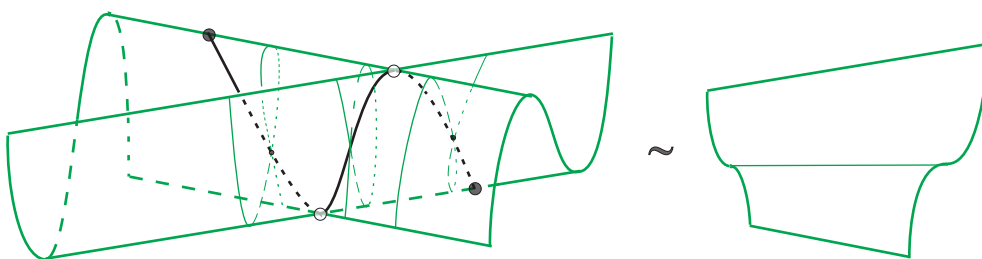




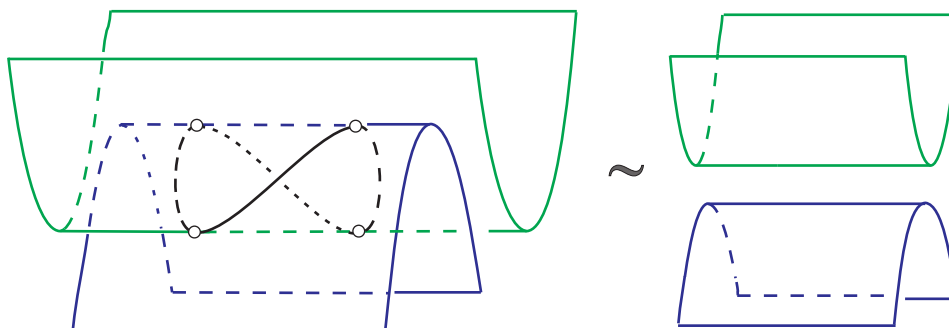
10iv: a move on surfaces associated to a cubic tangency \times



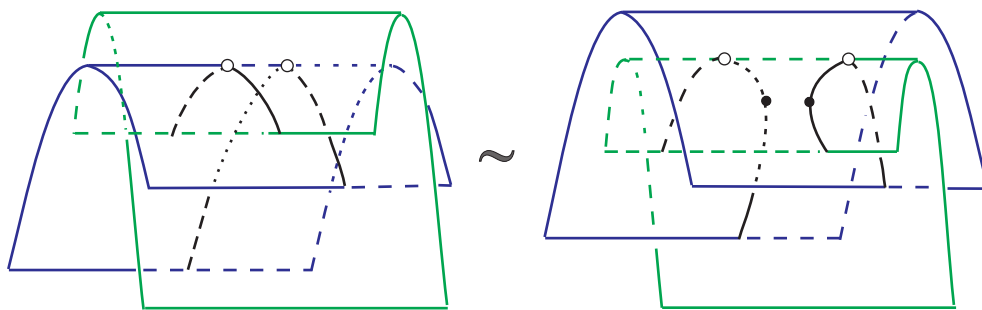
10v: a move on surfaces associated to a ramphoidal cusp \curvearrowright



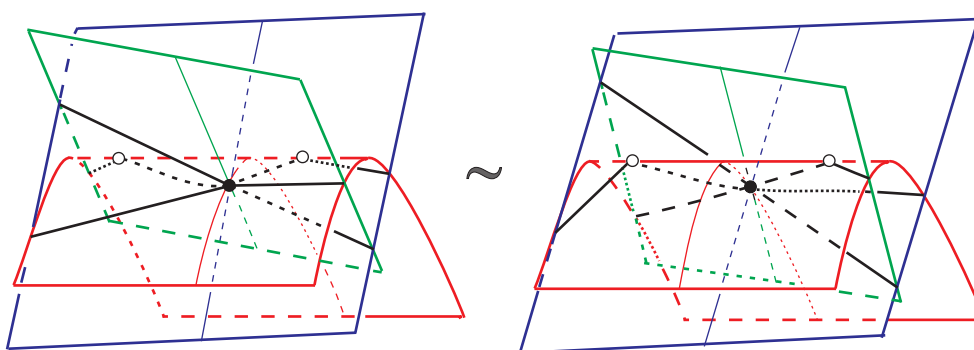
10vi: a move on surfaces associated to a horizontal cusp \curvearrowleft




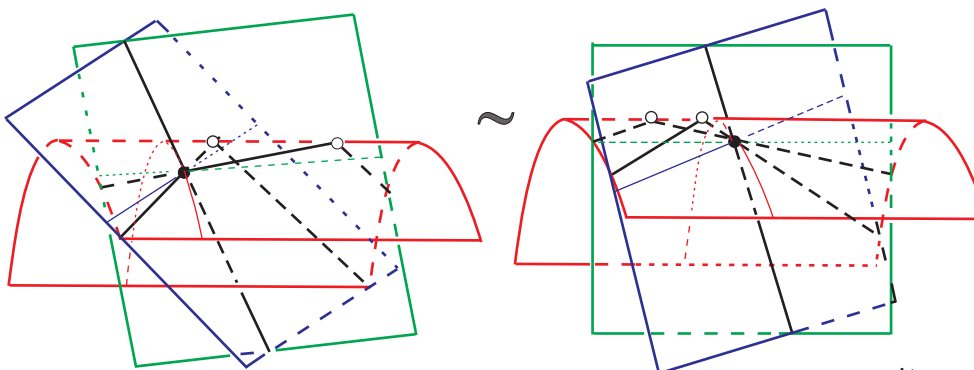
10vii: a move on surfaces associated to a mixed tangency \times



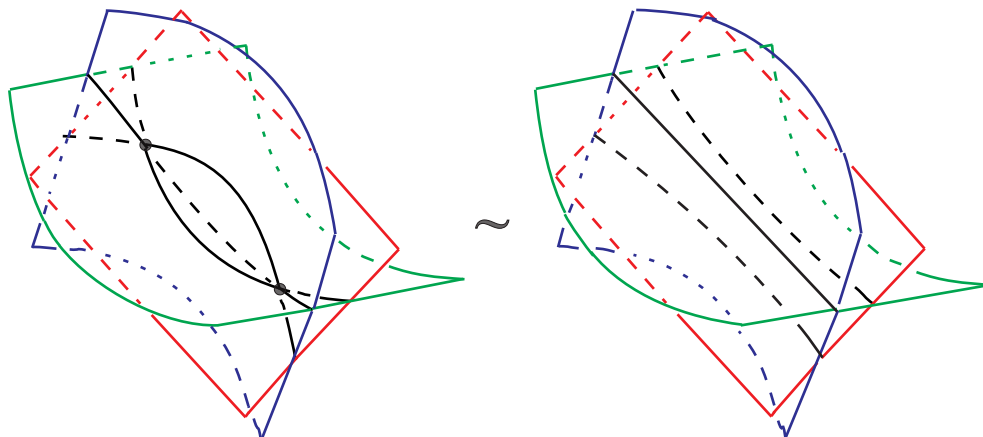
10viii: a move on surfaces associated to an extreme tangency 



10ix: a move associated to a horizontal triple point 



10x: a move associated to a horizontal triple point 



10xi: a move on surfaces associated to a tangency with 

Lemma 5.8. *Let L_0, L_1 be generic loops of links. If $\text{DS}(L_0)$ and $\text{DS}(L_1)$ are equivalent in the sense of Definition 5.4, then L_0 and L_1 are generically homotopic.*

Proof. Any equivalence of diagram surfaces gives rise to a smooth family of loops $\{L_r\}$ by Lemma 5.6b. The constructed family $\{L_r\}$ is a generic homotopy since all moves in Figure 10 correspond to singularities in the sense of Definition 3.4. \square

By Lemmas 5.7 and 5.8 the classification of generic links reduces to the equivalence problem for their diagram surfaces.

Proposition 5.9. *Generic links K_0, K_1 are generically equivalent if and only if the diagram surfaces $\text{DS}(K_0), \text{DS}(K_1)$ are equivalent in the sense of Definition 5.4.* \square

The isotopy class of a link can be easily reconstructed from its plane diagram, hence from its diagram surface with labels. Formally, one has the following.

Lemma 5.10. *Suppose that the diagram surface $\text{DS}(K)$ of a generic link K is given, but K is unknown. Then one can reconstruct the isotopy class of $K \subset V$.* \square

6. THE TRACE GRAPH OF A LINK AS A LINK INVARIANT

6.1. The trace graph of a link and generic trace graphs.

Here the classification of links $K \subset V$ will be reduced to their trace graphs.

Definition 6.1. Let $S \subset A_{xz} \times S_t^1$ be the diagram surface of a loop of links. The *trace graph* $\text{TG}(S)$ is the self-intersection of S , ie a finite graph embedded into $A_{xz} \times S_t^1$. The *trace graph* $\text{TG}(K)$ of a link K is the trace graph of its diagram surface $\text{DS}(K)$. The trace arcs of $\text{DS}(K)$ are called *trace arcs* of $\text{TG}(K)$. The trace graph inherits the vertices and labels from $\text{DS}(K)$. \blacksquare

Definition 6.2. A finite graph $G \subset A_{xz} \times S_t^1$ is *generic* if Conditions (i)–(ii) hold.

(i) **Conditions** on *trace arcs* and *vertices*.

- the graph G consists of finitely many *trace arcs*, which are monotonic arcs with respect to the orthogonal projection $\text{pr}_z : G \rightarrow S_z^1$;
- any endpoint of a trace arc of G has either degree 1 (a *hanging vertex* \bullet) or degree 2 (a *critical vertex* \bowtie);
- the critical vertices of G coincide with the critical points of $\text{pr}_z : G \rightarrow S_z^1$;
- trace arcs of G intersect transversally at *triple vertices* (\times);
- the critical points of $\text{pr}_z : G \rightarrow S_t^1$ are called *tangent vertices* (ζ).

(ii) **Conditions** on *labels*.

- each trace arc of G is labelled with a *label* $(q_i s_j)$ as in Definition 4.2;
- under $t \mapsto t + \pi$ the graph G maps to its image under the symmetry in S_z^1 ;
- under the time shift $t \mapsto t + \pi$ each label $(q_i s_j)$ reverses to $(s_j q_i)$;
- every triple vertex $v \in G$ is labelled with a *triplet* $(q_i s_j), (s_j r_k), (q_i r_k)$ consisting of the labels associated to the trace arcs passing through v ;
- each hanging vertex is labelled with the label of the corresponding trace arc;

- for any i and $q = 1, \dots, n_i$, there are exactly two hanging vertices of G labelled with $((q+1)_i, q_i)$ and $(q_i, (q+1)_i)$, respectively;
- at every critical vertex of G the labels of trace arcs may transform as follows: either $(q_i s_j) \leftrightarrow (q_i, (s \pm 1)_j)$ or $(q_i s_j) \leftrightarrow ((q \pm 1)_i, s_j)$. ■

A trace arc of a generic graph may consist of several edges in the usual sense.

Lemma 6.3. (a) *For any generic surface S , the trace graph $\text{TG}(S)$ is generic in the sense of Definition 6.2. So the trace graph $\text{TG}(K)$ of a generic link K is generic.*

Proof. Conditions (i)-(v) of Definition 5.2 imply Conditions (i)-(ii) of Def. 6.2. □

Definition 6.4. A smooth family of trace graphs $\{G_s\}$, $s \in [0, 1]$, is called an *equivalence* if there are finitely many critical moments $s_1, \dots, s_k \in [0, 1]$ such that

- for all non-critical moments $s \notin \{s_1, \dots, s_k\}$, the trace graphs G_s are generic;
- if s passes through a critical moment, G_s changes by a move in Figure 11. ■

The moves in Figure 11 should be considered locally, ie the diagrams do not change outside the pictures. Various mirror images of the moves are also possible. Moreover, some labels $s+1$ can be replaced by $s-1$ and vice versa. Trace graphs are symmetric under $t \mapsto t + \pi$, i.e. each move in Figure 11 denotes two symmetric moves. The most non-trivial moves are *tetrahedral* moves 11i and *trihedral* moves 11xi. Their geometric interpretation at the level of links is shown in Figure 12.

Notice that both moves in Figure 11i can be realized for links and closed braids. In general a tetrahedral move corresponds to a link or a braid with a horizontal quadrisecant. Geometrically two arcs intersect a wide band bounded by another two arcs. Under a tetrahedral move, the two intersection points swap their heights as in Figure 12. The first picture of Figure 11i applies when the intermediate oriented arcs go together from one side of the band to another like \Rightarrow . The second picture means that the arcs are antiparallel as in the British rail mark \Leftrightarrow . It is easier to understand Lemma 6.5 first for knots, when the indices $i, j = 1$ can be missed.

Lemma 6.5. (a) *For a generic trace graph G such that $G \cap (A_{xz} \times \{0\})$ are crossings of a general diagram, there is a generic surface S such that $\text{TG}(S) = G$.*

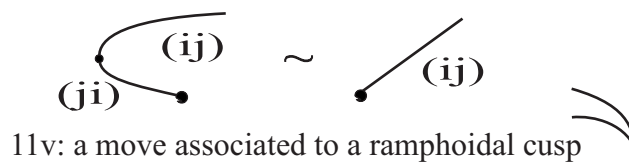
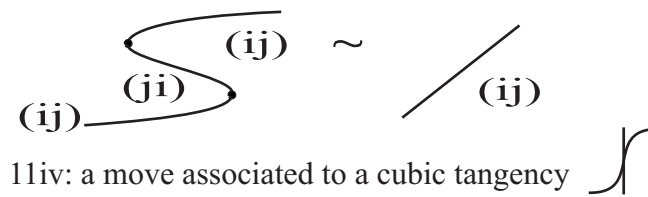
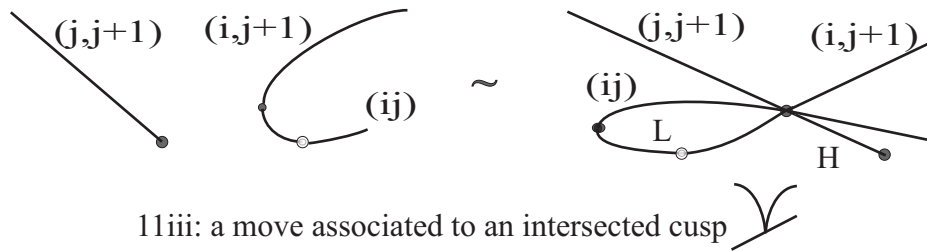
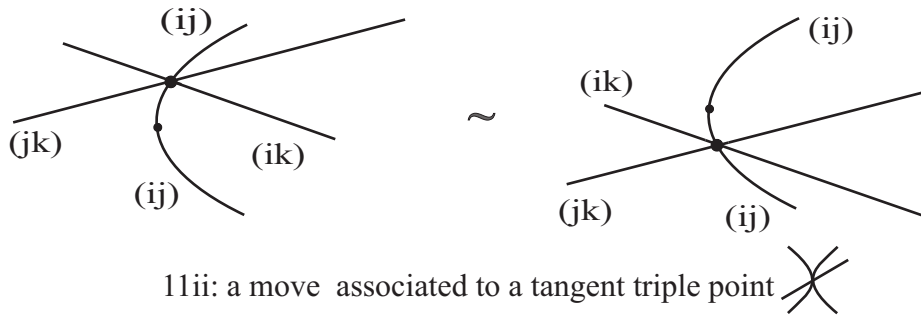
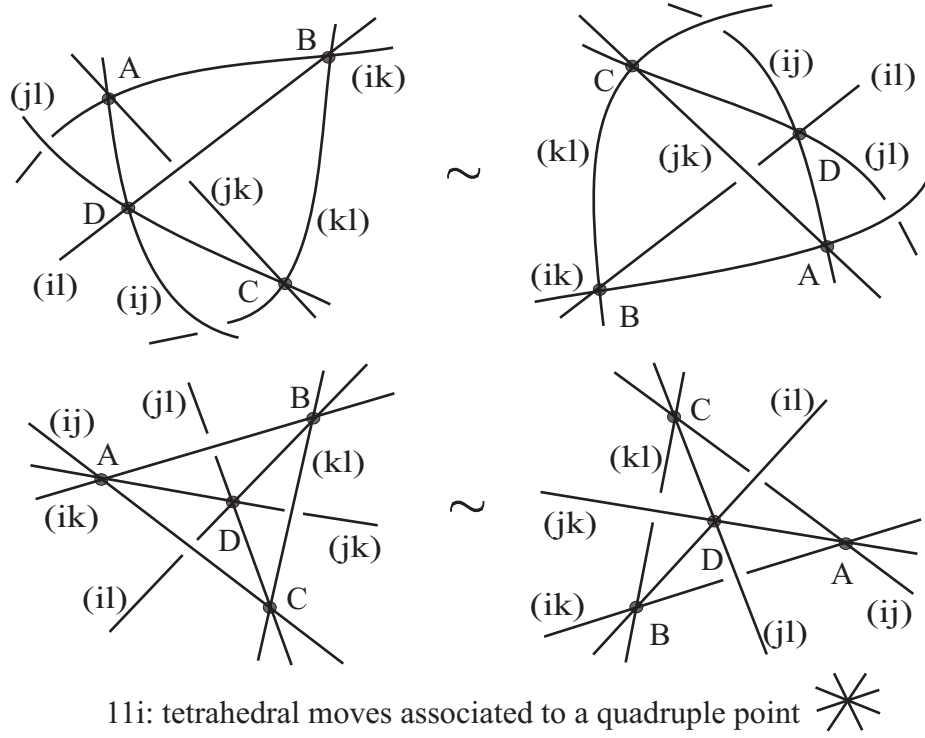
(b) *For any equivalence of trace graphs $\{G_r\}$, there is an equivalence of surfaces S_r with $\text{TG}(S_r) = G_r$, $r \in [0, 1]$.*

Proof. (a) Consider a vertical section $P_t = G \cap (A_{xz} \times \{t\})$ not containing vertices of G . Then P_t is a finite set of points with labels $(q_i s_j)$, where $i, j \in \{1, \dots, m\}$, see Definition 5.2. The points in P_t will play the role of crossings of sections of S .

The labelled set P_t defines the Gauss diagram GD_t as follows, see Definition 2.7. Take $\sqcup_{i=1}^m S_i^1$, split each circle S_i^1 into n_i arcs and number them by $1, \dots, n_i$ according to the orientation. We mark several points in the q -th arc of S_i^1 in a 1-1 correspondence and the same order with the points of P_t projected under $\text{pr}_z : P_t \rightarrow S_z^1$ and having labels $(q_i s_j)$ or $(s_j q_i)$, $s = 1, \dots, n_j$.

So each point of P_t gives 2 marked points in $\sqcup_{i=1}^m S_i^1$, labelled with $(q_i s_j)$ and $(s_j q_i)$. Connect them by a chord and get the Gauss diagram GD_t . The zero Gauss diagram GD_0 is realizable by the given general diagram. Hence all Gauss diagrams GD_t give rise to a family of diagrams D_t , ie to a surface $S = \cup(D_t \times \{t\})$.

(b) Apply the construction from (a) to each trace graph G_r , $r \in [0, 1]$. □



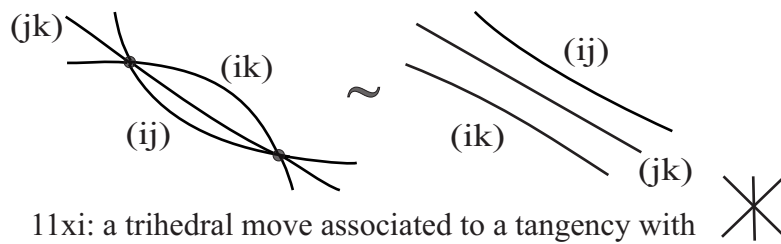
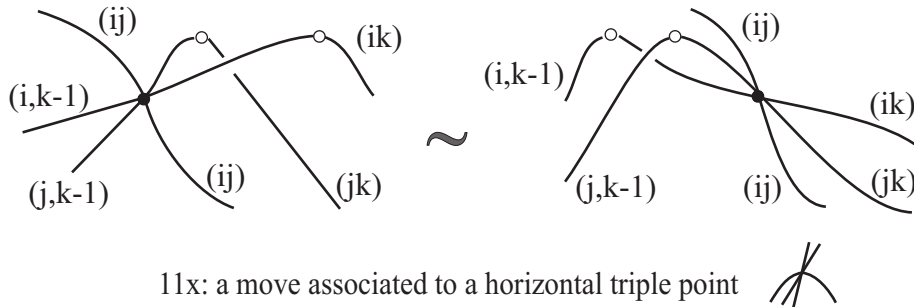
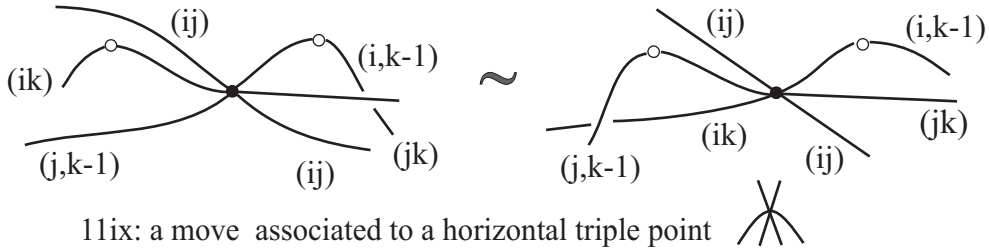
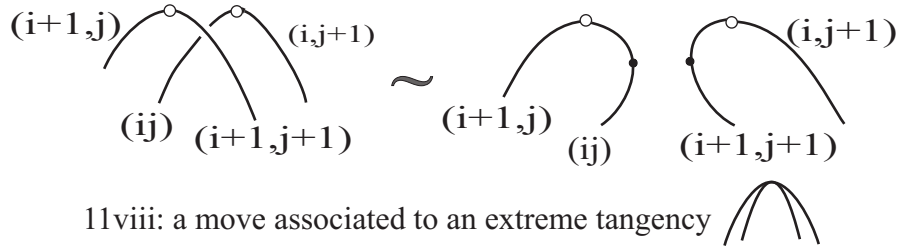
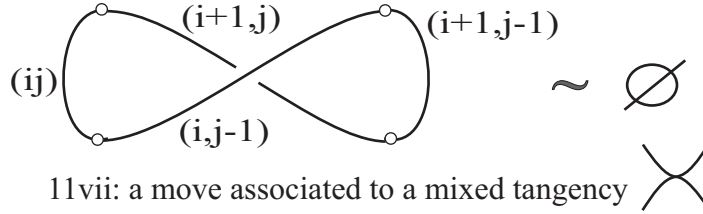
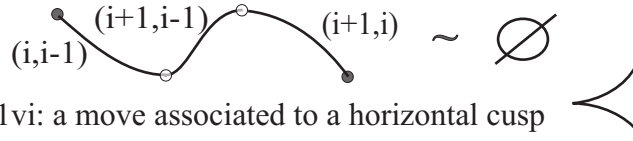


FIGURE 11. Moves on trace graphs

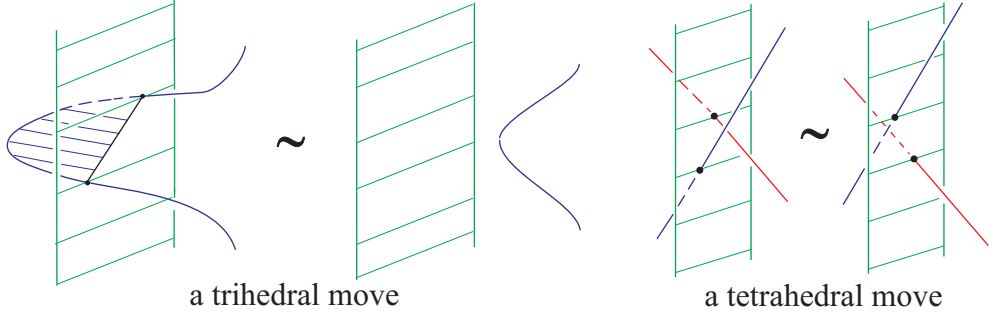


FIGURE 12. A trihedral move and a tetrahedral move for links.

Proposition 6.6. (a) *Trace graphs $\text{TG}(S_0), \text{TG}(S_1)$ of generic surfaces are equivalent in the sense of Definition 6.4 if and only if the surfaces S_0, S_1 are equivalent in the sense of Definition 5.4.*

(b) *Generic surfaces S_0, S_1 are equivalent in the sense of Definition 5.4 if and only if $\text{TG}(S_0), \text{TG}(S_1)$ are equivalent in the sense of Definition 6.4.*

Proof. (a), (b) Any equivalence $\{S_r\}$ of surfaces gives rise to the equivalence $\text{TG}(S_r)$ of trace graphs. Any equivalence of trace graphs gives rise to a smooth family of diagram surfaces $\{S_r\}$ by Lemma 6.5b. The family $\{S_r\}$ is an equivalence of diagram surfaces since the moves in Figure 11 are restrictions of the moves in Figure 10. \square

Theorem 1.4 directly follows from Propositions 3.8, 3.12, 5.9 and 6.6.

Lemma 6.7. *Suppose that the trace graph $G = \text{TG}(K)$ of a generic link K is given, but K is unknown. Then one can construct a generic link K' equivalent to K .*

Proof. Lemma 6.5a provides a generic surface S such that $\text{TG}(S) = G$. Due to labels of trace arcs, the section $D_0 = S \cap (A_{xz} \times \{0\})$ gives rise to a link $K' \subset V$ with $\text{pr}_{xz}(K') = D_0$. The link K' can be assumed to be generic by Proposition 3.8a and is equivalent to K since K and K' have the same Gauss diagram. \square

6.2. Combinatorial construction of a trace graph.

Lemma 6.8. *Let $K \subset V$ be a link with $2e$ extrema of the projection $\text{pr}_z : K \rightarrow S_z^1$ and l crossings in the diagram $\text{pr}_{xz}(K)$. Let the extrema and intersection points from $K \cap (D_{xy} \times \{z = \pm 1\})$ divide K into n arcs monotonic with respect to pr_z . Then K is isotopic in V to a link K' such that $\text{TG}(K')$ contains $2l(n-2)$ triple vertices, $4(n-e-1)e$ critical vertices and $2e$ hanging vertices.*

Proof. Take a generic link K' smoothly equivalent to K and having an isotopic plane diagram. We split K' by horizontal planes into several horizontal slices such that each slice contains exactly one crossing or one extremum with respect to $\text{pr}_z : K' \rightarrow S_z^1$. We may assume that all maxima are above all minima, otherwise deform K' accordingly. To each slice we associate the corresponding elementary trace graph and glue them together, see examples in Figure 13 and Figure 14.

Figure 13 shows two explicit examples for the opposite crossings in the braid group B_4 . In general we mark out the points $\psi_k = 2^{1-k}\pi$, $k = 0, \dots, n-1$ on the boundary of the bases $D_{xy} \times \{\pm 1\}$. The 0-th point $\psi_0 = 2\pi$ is the n -th point.

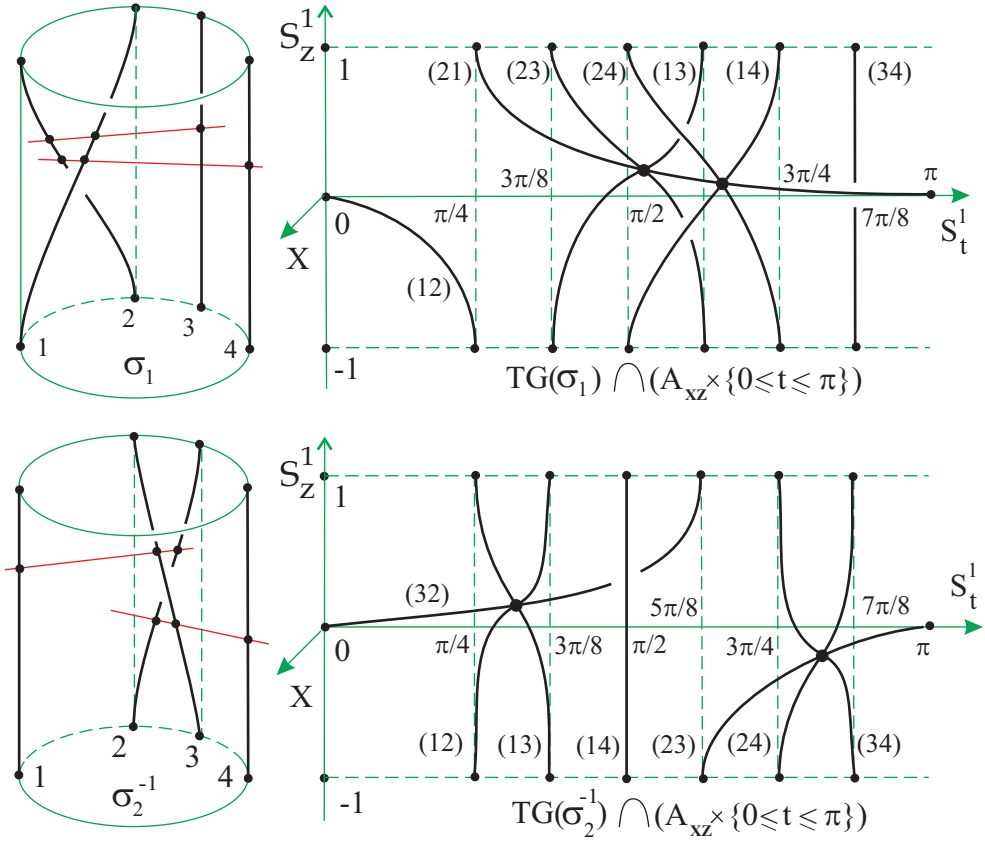
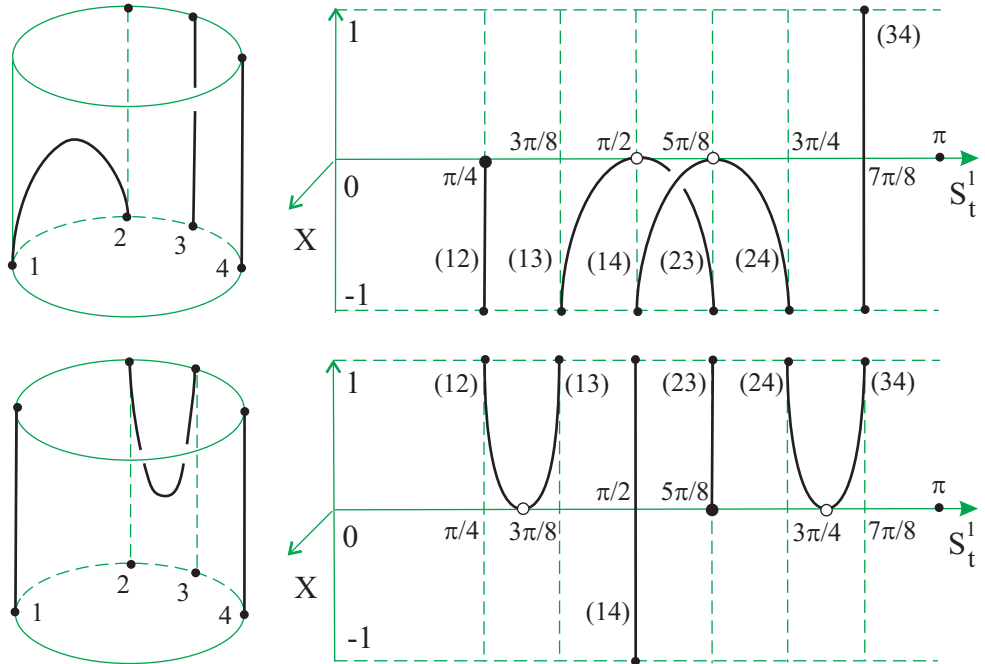
FIGURE 13. Half trace graphs of the 4-braids $\sigma_1, \sigma_2^{-1} \in B_4$.

FIGURE 14. Half trace graphs of elementary blocks containing extrema.

The crucial feature of the distribution $\{\psi_k\}$ is that all straight lines passing through two points ψ_j, ψ_k are not parallel to each other. Firstly we draw all strands

in the cylinder $\partial D_{xy} \times [-1, 1]_z$. Secondly we approximate with the first derivative the strands forming a crossing by smooth arcs, see the left pictures in Figure 13.

Then each elementary braid σ_i constructed as above has exactly $n - 2$ horizontal trisecants through the strands $i, i + 1$ and j for $j \neq i, i + 1$. Each trisecant is associated to a triple vertex of the trace graph, see 4 horizontal trisecants in the left picture of Figure 13. The trace graphs in Figure 13 are not generic in the sense of Definition 6.2, eg parallel strands 3 and 4 lead to the vertical trace arc labelled with (34). But we may slightly deform such a trace graph to make it generic.

In the first picture of Figure 14 the arc with a maximum is the intersection of the cylinder $\partial D_{xy} \times [-1, 1]_z$ with an inclined plane containing the straight line 1-2 in the base $D_{xy} \times \{-1\}$. The highest maximum of K' leads to exactly $2(n - 2e)$ critical vertices (with symmetric images under $t \mapsto t + \pi$), the next maximum gives $2(n - 2e + 2)$ critical vertices and so on, i.e. the total number is $2(n - 2e) + 2(n - 2e + 2) + \dots + 2(n - 2) = 2(n - e - 1)e$. The number of critical vertices associated to minima of K' is the same. Moreover each of $2e$ extrema gives one hanging vertex. \square

REFERENCES

- [1] V. Arnold, A. Varchenko, S. Gusein-Zade, *Singularities of Differentiable Maps*, Moscow, 1982.
- [2] J. Birman, *Braids, Links and Mapping Class Groups*, Ann. of Math. Studies 82, Princeton University Press, 1974.
- [3] J. Birman, V. Gebhardt, J. González-Meneses, *Conjugacy In Garside Groups I, II, III*, math.GT/0605230, math.GT/0606652, math.GT/0609616.
- [4] J. Damon, *The Unfolding and Determinacy Theorems for Subgroups of A and K*, Mem. Amer. Math. Soc. v. 50 (1984), no. 306.
- [5] J. M. S. David, Projection-generic Curves, J. London Math. Soc. (2), v. 27 (1983), 552–562.
- [6] T. Fiedler, *Gauss Diagram Invariants for Knots and Links*, Mathematics and Applications, v. 532, 2001, Kluwer Academic Publishers.
- [7] T. Fiedler, *One-Parameter Knot Theory* (117 pages), preprint, March 2003.
- [8] T. Fiedler, V. Kurlin, *Recognizing Trace Graphs of Closed Braids*, arXiv:0808.2713.
- [9] F.A. Garside, *The Braid Group and Other Groups*, Quart. J. Math. Oxford(2) v. 20 (1969), p. 235–254.
- [10] J. González-Meneses, *The n-th Root of a Braid is Unique up to Conjugacy*, Algebraic and Geometric Topology, v. 3 (2003), p. 1103–1118.
- [11] K. H. Ko, J. W. Lee, *A Fast Algorithm to the Conjugacy Problem on Generic Braids*, math.GT/0611454.
- [12] S. Mancini, M. A. S. Ruas, *Bifurcations of Generic One Parameter Families of Functions on Foliated Manifolds*, Math. Scand. 72 (1993), no. 1, 519.
- [13] K. Murasugi, *On Closed 3-Braids*, Memoirs of Amer. Math. Soc., v. 151, 1974.
- [14] C. T. C. Wall, Projection Genericity of Space Curves, J. of Topology, v. 1 (2008), 362–390.

LABORATOIRE EMILE PICARD, UNIVERSITÉ PAUL SABATIER, 118 ROUTE NARBONNE, 31062 TOULOUSE, FRANCE

E-mail address: fiedler@picard.ups-tlse.fr

DEPARTMENT OF MATHEMATICAL SCIENCES, DURHAM UNIVERSITY, DURHAM DH1 3LE, UNITED KINGDOM

E-mail address: vitaliy.kurlin@durham.ac.uk